Influence of soundboard modelling approaches on piano string vibration

Pablo Miranda Valiente, Giacomo Squicciarini, David J. Thompson

Institute of Sound and Vibration Research, University of Southampton, Southampton, SO17 1BJ, United Kingdom

This work explores the influence of the dynamics of the piano soundboard on string vibration and on the force acting between the vibrating string and the bridge. Four different soundboard representations of different complexity are considered: (i) a finite element model that considers the complete dynamic behavior of the soundboard at the connection point with the string within the frequency range of interest, (ii) a reduced modal model containing only five modes, (iii) a Kelvin-Voigt system characterized by an equivalent stiffness and damping and (iv) a rigid soundboard represented by a simply supported boundary condition. The connection between the string and the soundboard is modelled by coupling a simply supported stiff string model with the different representations of the soundboard through a contact stiffness. As well as directly accounting for the string-soundboard coupling, this approach also includes the duplex scaling segment. The latter can be left to vibrate freely or muted with a continuous distribution of dampers. Although the simplest soundboard representation is not dissimilar from the other more complex models, the dynamics of the soundboard affect the decay time of the note, the force transmitted to it, and the vibration of the radiating surface of the soundboard.

I. INTRODUCTION

The strings of musical instruments, including the piano, are generally coupled through a bridge to a soundboard, which radiates sound more efficiently. The vibration of the strings is affected by this coupling to some extent. The bridge and soundboard provide a quasi-rigid termination to the string at its speaking length, allowing it to vibrate at its fundamental frequency and associated harmonics. Although most of the vibration energy is reflected back into the string, parts are also transmitted into the soundboard and past the bridge into the duplex scaling segment of the string[1]. The connection with the soundboard can also produce the double polarization of the strings[2], and can provide coupling between vertical and longitudinal directions.

In the literature, the connection between the strings and the soundboard has been modelled either by studying the dynamics of two separate systems or, less frequently, by accounting for a full coupling between them. When the string and the soundboard are modelled as decoupled systems, the component of the string tension perpendicular to the soundboard serves as an input to the vibration of the soundboard[3-6]. In these cases, the length of the string corresponds to the distance between the agraffe and the bridge (the speaking length, i.e., neglecting the duplex scaling segment), and its ends are simply supported. String vibration excited by the hammer can then be studied with numerical approaches such as finite differences[7-11]. In a fully coupled approach, however, the dynamics of the soundboard at the bridge provides a non-rigid boundary for the string. In this case the total length of the string between the agraffe and the hitch pin is included. Models of this type are more complex but can better explain the effect of the soundboard on the string vibration and hence on the force transmitted to the soundboard. Fully coupled string-soundboard models for piano acoustics have been proposed by the authors[12;13] and also exist for other instruments[14-17]. Finite difference approaches[14] or modal models in the time domain[15-17] have been successfully implemented to obtain the string vibration and contact forces of the coupled system.

Whether they are seen as part of a coupled system or as independent vibrating components, the strings and soundboard can be represented using different modelling techniques. For string vibration, the equation of a stiff string solved with Finite Differences is probably the most popular method in musical acoustics but Finite Elements (FE)[5] or modal models have also been presented[16;17]. The dynamics of the soundboard at the bridge have been addressed in different ways, including a frequency-dependent boundary condition for string-only models[18], or plate models such as thin plates[4], Reissner-Mindlin plates[5] (including shear deformations), linear filters[19] or FE[20-22]. The soundboard itself was characterized experimentally at the bridge by Wogram[23], using different modal analysis techniques. The coupled vibration of the string soundboard system was analyzed, and it was found that the decay of string tones was larger due to the reduced energy transfer caused by the mismatch in the impedance. Ege et al.[24] characterized the soundboard both numerically and experimentally. Among other things the authors studied the nonlinear behavior of the soundboard which was quantified to be orders of magnitude smaller than the linear one. Their study also gives an insight into the damping of the soundboard. Values of damping ratio between 0.005 and 0.015 were obtained. Similar values for the soundboard damping were obtained by Corradi et al.[25]. These authors measured the vibration of the soundboard at different manufacturing stages and noted that, at advanced manufacturing stages the soundboard presents damping ratios varying between 0.008 and 0.03. In Squicciarini's thesis[21], the finished soundboard fitted into the piano exhibited even higher damping ratios ranging between 0.007 and 0.047. Suzuki[26] obtained values of 0.032 for the first mode and between approximately 0.01 and 0.015 for higher modes, while Berthaut[27] obtained smaller values of $0.003 - 0.0065$.

Trevisan et al.[28] developed analytical soundboard models, in which the soundboard was modelled as a Love-Kirchhoff plate. One of the interesting conclusions reached by the authors is that geometric and manufacturing details of the soundboard can have an influence on the first natural frequencies

when compared with experimental results. Closely related to the present study, reduced soundboard modelling has been introduced by various authors, see for instance Boutillon & Ege[29], and Corradi et al.[25]. In these studies, the frequency response of the soundboard is approximated in an average sense by combining the driving point impedances of an infinite beam and an infinite plate. These approaches were formulated directly in the frequency domain and cannot be directly adopted in a time-domain solution.

The main aim of this work is to develop a model of a coupled system, in which a piano string and soundboard are connected at the bridge, and to evaluate the degree of complexity required to describe the dynamic behavior of the soundboard. For this purpose, different dynamic models of a soundboard, of increasing complexity, are coupled to a string in the direction perpendicular to the soundboard, as described in Section II. The authors have previously developed models using one of the simpler soundboard representations to study the dynamics of the coupled system in two[12] and three[13] directions. Differently from this, in the current work comparisons are made between different soundboard models which focus on the transverse direction perpendicular to the soundboard. To calculate the response of the coupled system, a time-domain model in a state-space formulation is implemented in Section III. This approach requires the structural damping of the string alone, for which an experimental setup is designed, and measurements are performed in Section IV to determine the damping of strings disconnected from the bridge. The implications of using the different soundboard representations are discussed in Section V, with conclusions given thereafter. The modelling approach considers only the transverse direction perpendicular to the soundboard, and no nonlinear phenomena are considered such as the generation of phantom partials due to the coupling between transverse and longitudinal directions on the strings[19]. Instead, the main novelty of this work lies in the exploration of the details needed to model the soundboard to account for the interaction with the string. Furthermore, the inclusion of a duplex scaling

segment in the model, which can be either be attenuated with a continuous distribution of dampers and springs or left free to vibrate (see below), is an aspect that, to the best of the authors' knowledge, has not been extensively addressed before.

II. STRING AND SOUNDBOARD

A string of length L connected to a soundboard system is shown in Figure 1 together with the main variables adopted for the analysis. These are the displacements y and forces F, at the hammer striking point e from a distance L_e from the agraffe termination, and at the connection points between the string s and soundboard b. Only vibration perpendicular to the soundboard is considered; this direction will be referred to as vertical. The connection with the soundboard divides the string of total length L into two parts, the speaking length L_s and the remaining vibrating duplex scaling segment L_d. With the aim of analyzing the effect of soundboard dynamics on the string vibration and transmitted force, three different representations of the soundboard are developed and compared in the following sections. These are also summarized schematically in Figure 1 and are a full modal FE model, a reduced modal model and a Kelvin-Voigt system. A contact stiffness k_c is introduced to represent the normal contact stiffness associated with local deflection at the contact point. Although the contact stiffness could be accounted for implicitly by higher order modes in the modal summation of the soundboard mobilities presented in section II-B, it is not considered as the modal summations are truncated. In addition a simply supported end at the bridge location (i.e. rigid soundboard) is considered.

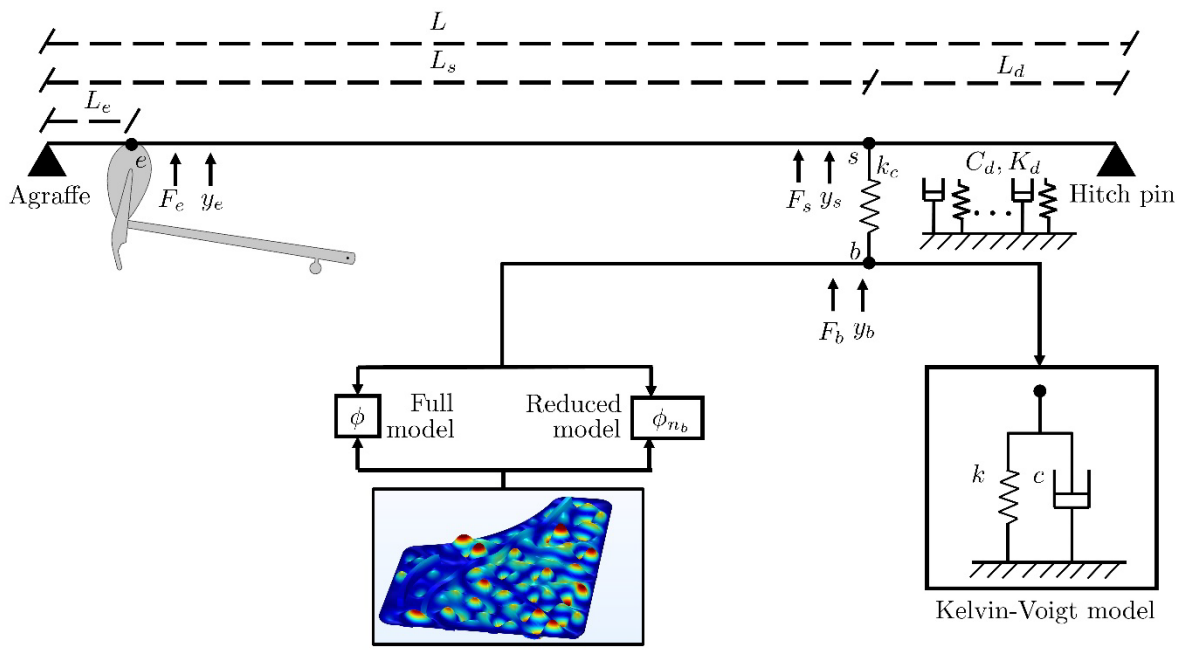

Figure 1. (color online) Schematic representation of a string coupled with different representations of the soundboard. These are a full FE model, a reduced modal model and an equivalent Kelvin-Voigt system.

A. Stiff string model

A model is defined for the vertical motion of the string uncoupled from the soundboard and simply supported at its ends defined by the agraffe and hitch pin (see Figure 1). It is represented as a stiff string with an equation of motion given as[30]:

$$\mu \frac{\partial^2 y}{\partial t^2} = T_0 \frac{\partial^2 y}{\partial x^2} - ESK^2 \frac{\partial^4 y}{\partial x^4} \tag{1}$$

where y is the vertical motion of the string in a position x across the string at a time t, μ is the mass per unit length, T_0 is the tension, E is the Young's modulus, S is the cross-sectional area and K is the radius of gyration. For a pinned string with length L, the n-th mode shape at a position x from the agraffe and the corresponding natural angular frequency are[30]

$$\phi_n(x) = sin(n\pi x/L)\,, \qquad \omega_n = n2\pi f_0(1 + Bn^2)^{\frac{1}{2}} \tag{2}$$

where $f_0 = (T_0/\mu)^{\frac{1}{2}}/2L$ is the fundamental frequency of the string in the absence of bending stiffness, and the inharmonic coefficient $B = \pi^2 ESK^2/T_0L^2$. Damping is omitted from Eq.(1) but this will be included in terms of damping ratios (see Section III) in the state-space formulation and also indirectly by coupling with the soundboard.

In a coupled string-soundboard system the force at the bridge is calculated from the interaction between the two components as outlined below. In the absence of a soundboard model (i.e., simply supported string at the bridge) the input force can be written considering the vertical component of the tension and a third order derivative related to the bending stiffness, evaluated at the string termination $x = L_s$, as:

$$F_{ss} = -T_0 \left.\frac{\partial y}{\partial x}\right|_{x=L_s} + ESK^2 \left.\frac{\partial^3 y}{\partial x^3}\right|_{x=L_s} \tag{3}$$

B. Soundboard Models

The different soundboard models adopted in this work are introduced in this subsection. These are an FE model, a reduced modal soundboard the response of which is fitted to the FE model and a Kelvin-Voigt soundboard consisting of a spring-damper system.

1. FE model

The geometry of the soundboard adopted in this work is based on a grand piano that was made available to the authors. An FE model that can represent the complete soundboard dynamics has been developed in COMSOL Multiphysics®. The thickness of the soundboard varies between 7 and 9 mm from the edge to the center; its edges are clamped, the bridges and the wooden stiffener beams - often referred to as ribs - are modelled as isotropic and the soundboard as orthotropic. The

assumption of isotropic ribs and bridges is justified from previous studies by one of the coauthors[21], in which a design sensitivity analysis was performed. It was found that the most important parameter of the ribs is the Young's modulus in their longitudinal direction, with their other directions being negligible. This matches the purposes of the ribs, which are to stiffen the soundboard in its weakest direction. The properties of the wood correspond to Sitka spruce and were obtained from literature[21], but the stiffest direction of the Young's modulus and the density have been modified to provide a better agreement with driving point mobility measurements. The direction convention used for the material properties is illustrated in Figure 2, along with the points at which the mobilities are obtained along the two bridges. Additionally, a point k is identified in the middle of the soundboard that is used to compute the vibrational response as described in section IV, C. Regarding the mesh, approximately 49000 quadratic tetrahedral elements were used with a minimum size of $\frac{\lambda_{pl}}{9}$ in the ribs and the bridge and $\lambda_{pl}/10$ in the soundboard, with λ_{pl} being the shortest wavelength of a simple Kirchhoff plate representing the soundboard. The ribs/bridge and soundboard are considered as elastic bodies which share common element nodes, corresponding to a perfect connection between the domains. The main parameters of the model are listed in Table 1. The first three modes calculated using the FE model are shown in Figure 3.

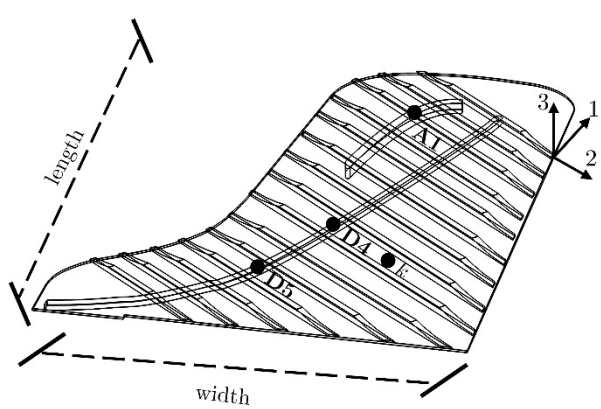

Figure 2. Overview of soundboard geometry, with locations of connection points for each note and response point k. Conventions used for directions of orthotropic properties of wood are also shown.

Table 1: Parameters of FE soundboard model

Description	**Value**	**Units**	**Description**	**Value**	**Units**
Soundboard width	1.39	m	Poisson's ratio, ν_{12}	0.37	–
Soundboard length	1.66	m	Poisson's ratio, ν_{13}	0.47	–
Young's modulus, E_1	17.1	GPa	Poisson's ratio, ν_{23}	0.43	–
Young's modulus, E_2	1.04	GPa	Shear modulus, G_{12}	1.0	GPa
Young's modulus, E_3	0.48	GPa	Shear modulus, G_{13}	0.96	GPa
Thickness	0.007 – 0.009	m	Shear modulus, G_{23}	0.04	GPa
Density	600	$\mathrm{kg/m^3}$			

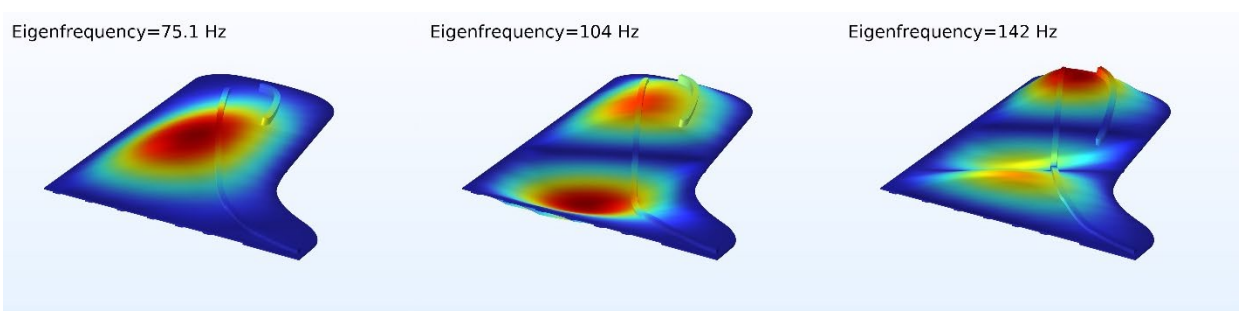

Figure 3. (color online) First three modes of the soundboard calculated using FE.

To calibrate the FE model, measurements of the mobility were performed. Impact testing was conducted using an impact hammer PCB model 086C03, sensitivity: (±15%) 2.25 mV/N,

measurement range: ±2224 N pk, hammer mass: 0.16 kg. The response was obtained using a miniature uniaxial accelerometer PCB model 352C23, sensitivity: (±15%) 1.0 mV/(m/s^2). Both devices were connected to a Data Physics Quattro, a portable Data Acquisition System.

A coherence above 0.9 was achieved for frequencies between 50 and 4000 Hz. Damping ratios of the first six modes were estimated from the measured mobilities, using the circle fitting procedure[31]. These are shown in Table 2. For higher frequencies, damping was chosen to represent the different behavior that the piano structure may have on the mobility response.

Table 2: Measured damping ratios.

Natural frequency, Hz	**Damping ratio**
75.0	0.04
118.8	0.034
145.3	0.019
182.8	0.024
242.2	0.025
260.9	0.018

To cover a frequency range between 50 and 4000 Hz, 800 modes of the soundboard are included in the modal summation. The measured driving point mobility at the bridge location of note D4 is compared with the results of the FE model in Figure 4. The FE model gives a similar trend and level of the mobility magnitude and phase and can be considered as a realistic representation of a piano soundboard. It is therefore used in this work as a reference result for the other simplified representations of the soundboard dynamics.

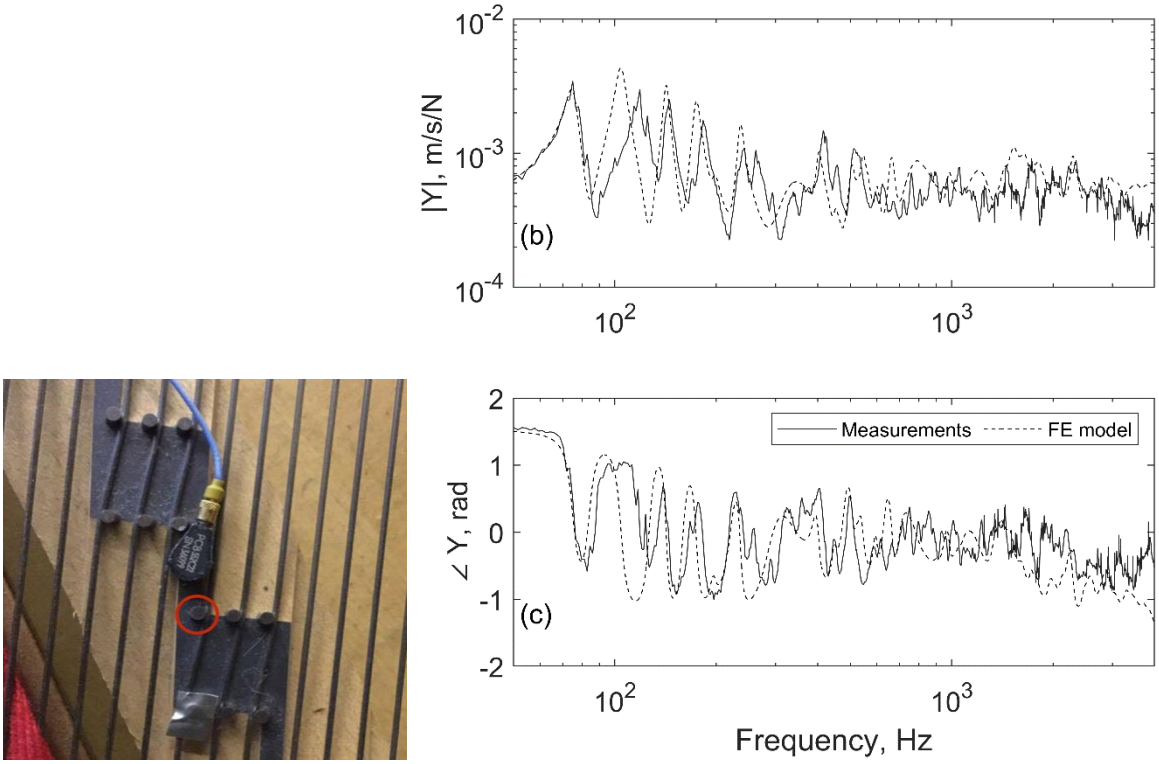

Figure 4 (color online). Left: Location of measurement, the impact point is circled in red. Right: Point mobilities of the soundboard at the bridge location corresponding to note D4. (b) Magnitude, (c) phase.

2. Reduced modal soundboard

A simpler model of the soundboard is developed using an equivalent modal system. Five modes are considered sufficient to represent the main low frequency resonances as well as the high frequency trends. The modal parameters of this equivalent system are determined by fitting the mobility to that from the FE model such that the first four modes capture the first four resonances while the fifth mode is more highly damped to represent the average level of the soundboard mobility at higher frequencies. Although it would be possible to extract the modal parameters directly from the FE model to yield correct natural frequencies and mode shapes, this would not produce the highly damped mode at higher frequencies that represents the overall trend of the mobility in this region. A

modal fitting approach is therefore applied by adopting the non-linear least squares curve fitting routine in MATLAB to refine the modal parameters of the reduced model and hence minimize the error between the FE mobility and the modal summation based on the five modes. The mass normalized mode shapes, damping ratios and natural frequencies are then obtained. The soundboard mobilities obtained at the bridge positions corresponding to notes A1, D4 and D5 are shown in Figure 5, together with those from the full FE model and the simplified approach discussed below. The reduced modal model can replicate both the dynamic behavior of the main modes and the average flat response at higher frequency. This can represent the mobilities quite well. However, at higher frequencies the reduced modal model can only represent the average behavior of the mobility. Alternative methods have been adopted in the literature[25;29;32] based on the mean value method proposed by Skudrzyk[33], although these can approximate the dynamic response of a complex structure in the frequency domain they cannot be directly used in time domain whereas the reduced modal model adopted in this study is well suited to provide a direct structural coupling between the string and the soundboard.

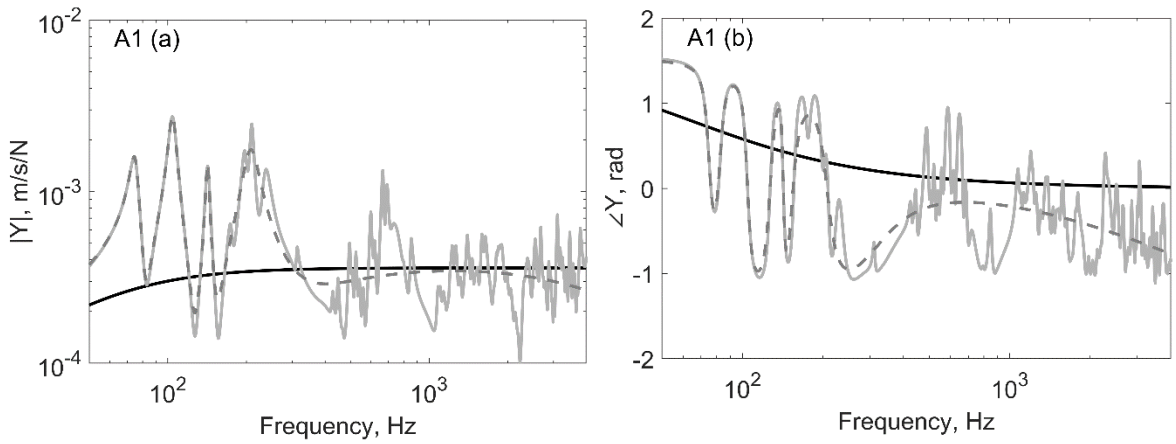

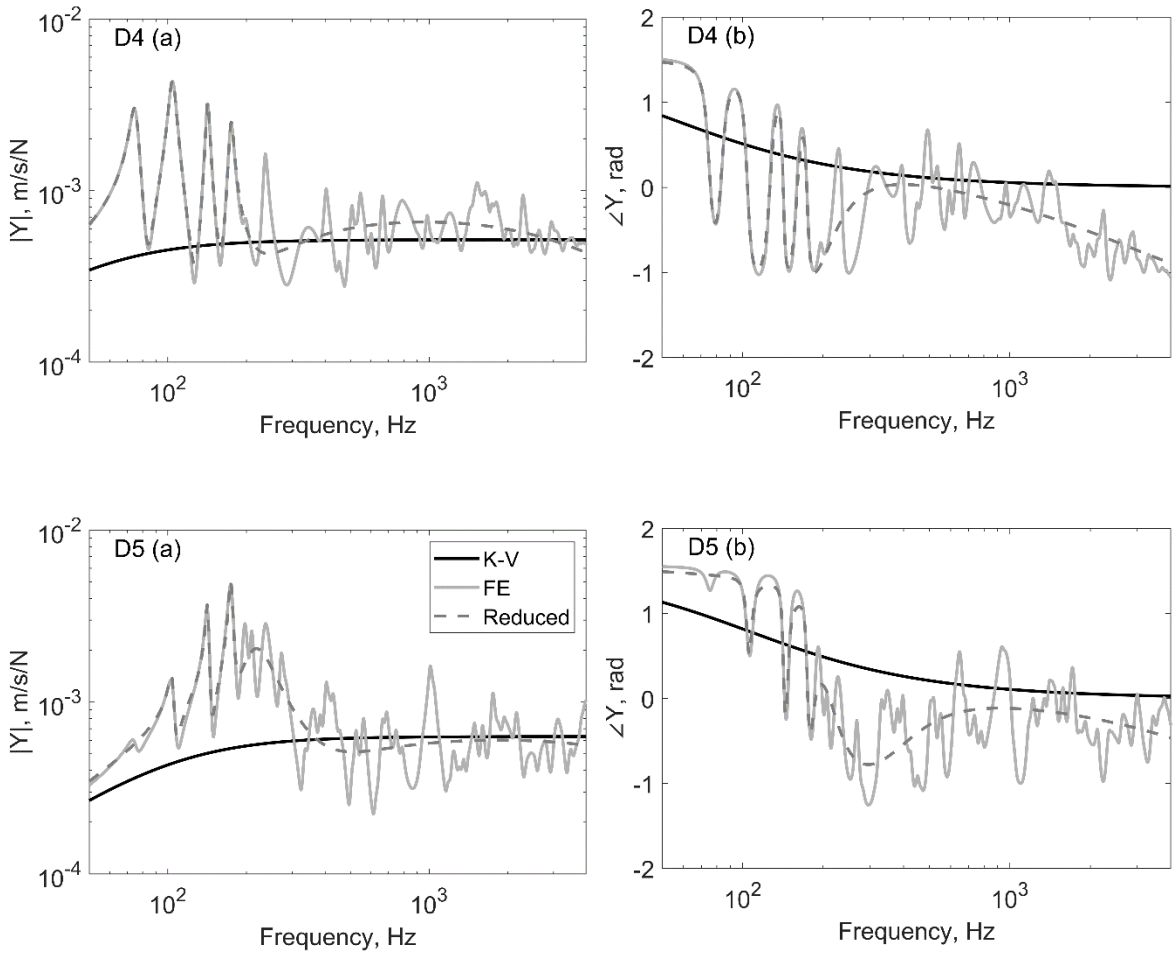

Figure 5. Soundboard mobilities obtained using different models at different locations. (a) Magnitude, (b) phase.

3. Kelvin-Voigt model for the soundboard

Since the soundboard is significantly stiffer than the strings[34], it may be sufficient to use a model that represents the generic trends and average values of the soundboard mobility without including the full modal characteristics. The local dynamic behavior of the soundboard is therefore modelled using a spring and a damper connected in parallel, which are tuned to fit to the mobility of the FE model. The stiffness is obtained from the low frequency asymptote where the model is stiffness-controlled. The spring constant k is hence obtained by considering the reference FE mobility Y_{FE} evaluated at a frequency ω_1 that needs to be 10 times smaller than the first natural frequency of the

soundboard. In this case $k = |j\omega_1/Y_{FE}(\omega_1)|$. The damper coefficient is obtained through the logarithmic average of the mobility at frequencies above 2500 Hz. The soundboard mobility obtained using this Kelvin-Voigt (K-V) approach is also shown in Figure 5. The spring-damper system can approximate the main trends but does not replicate the modal behavior.

To connect the K-V soundboard model to the string via the contact stiffness, a small mass is added at the interface to avoid numerical problems in the time-domain calculation. This mass should be small enough to ensure that the added mode is outside the frequency range of interest, since the trend of the mobility is chosen to be determined by the spring and damper only in this case.

4. Input force to the soundboard

The connection between the string and the soundboard is modelled by means of a contact stiffness which represents the local stiffness behavior at the contact point[15;16]. This method of connecting dynamic components of a system is also used in other areas research, such as railway noise and vibration research[35]. In the present case, the force is proportional to the relative displacement between string and soundboard as

$$F_b = k_c(y_s - y_b) \tag{4}$$

where y_s and y_b are the displacement of the string and soundboard at the bridge which can be obtained using the output state-space matrix $\mathbf{C}$ defined in section III-C, and k_c represents the stiffness of the contact zone. An expression for the contact stiffness k_c is derived starting from Hertzian contact theory [36]. For contact between cylindrical bodies, the normal load per unit length P acting over a contact patch of width a can be written as[36]

$$P = \frac{\pi E^* a^2}{4R} \tag{5}$$

where R is the equivalent radius of curvature for the two surfaces. For a cylinder in contact with a flat surface, representing the case of a string in contact with the bridge's surface, this is equivalent to the radius of the string alone. The equivalent Young's modulus E^* is given by:

$$E^* = \frac{E_s E_w}{E_s(1-\nu_w^2) + E_w(1-\nu_s^2)} \tag{6}$$

where E_s, ν_s and E_w, ν_w are the Young's moduli and Poisson's ratios of the steel string and the wooden bridge, the latter corresponding to E_3 in Table 1. Such an approximation considers the rigidity of the material in the direction normal to the surface.

Using a contact width $a \approx \sqrt{Rd}$, where d is the indentation and multiplying Eq.(5) by the length of the contact surface L_c gives the contact force as also derived by Popov[37]:

$$F_c = \frac{\pi L_c E^*}{4} d \tag{7}$$

from which the contact stiffness (F_c/d) is:

$$k_c = \frac{\pi L_c E^*}{4} \tag{8}$$

where L_c is the length of the contact zone. The value of k_c is in the order of $L_c E_w$ and for a small contact length $L_c \approx 0.01$ m is evaluated as 4.8×10^6 N/m.

The mobility of the soundboard obtained from the FE model at D4 is compared with that of the corresponding string (full length L) and contact stiffness in Figure 6. The soundboard mobility is on average five-to-six orders of magnitude smaller than that of the string at its resonances. The low structural damping of the string gives pronounced peaks and dips, unlike in the soundboard where the damping of the material is much higher. Consequently, at some antiresonances of the string, its

mobility is comparable or even lower than the soundboard and contact mobilities. The contact spring mobility exceeds that of the soundboard for frequencies above about 600 Hz. Results for the other notes exhibit similar trends, however for the A1 the spring mobility from 300 Hz exceeds that of the corresponding soundboard.

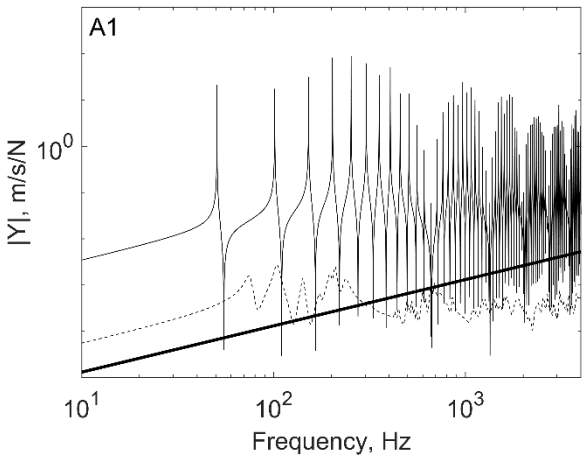

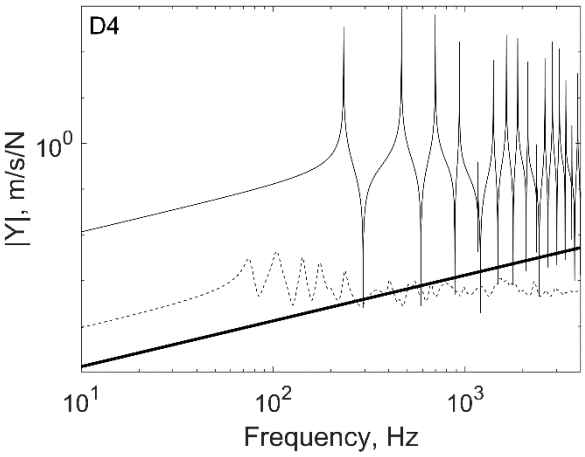

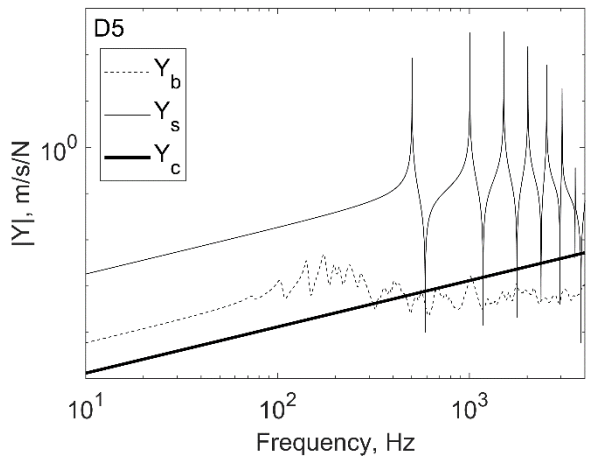

Figure 6. Mobility of the soundboard (FE model) Y_b, the string Y_s and contact stiffness Y_c for A1, D4 and D5.

III. TIME-DOMAIN MODEL

This section describes the state-space formulation adopted to represent and solve the dynamics of the coupled system in the time domain. The model adopted for excitation by the hammer is described first and this is followed by the state-space formulation of the coupled string-soundboard-hammer system. A brief discussion on the numerical scheme used for this study is given at the end of the section.

A. Hammer excitation

Since Ghosh in 1932 [38], different authors have modelled and showed experimentally that the hammer felt compression force is nonlinear and can be represented as a power law [7 39 40] given by:

$$F_e = K_H \xi^p, \tag{9}$$

while the equation of motion of the hammer can be written as:

$$F_e = -m_H \ddot{y}_H. \tag{10}$$

The parameters K_H, m_H and p correspond to the nonlinear stiffness, mass and power law coefficients obtained experimentally for piano hammers[41]. The term $\ddot{y}_H$ is the hammer acceleration while ξ is the compression of the hammer which can be expressed as:

$$\xi = \begin{cases} y_H - y_e & \text{if } y_H > y_e \\ 0 & \text{otherwise} \end{cases} \tag{11}$$

where y_H and y_e are the displacement of the hammer and the string at the excitation point, respectively.

Other approaches have been developed for the hammer-string interaction which can include, for example, the effects of hysteresis[42]. However, as the main focus of this analysis is the string-soundboard interaction, the simple power law formulation is adopted.

B. String coupled with soundboard

When the string is connected with any soundboard representation, the equations of motion of the system in state-space form can be expressed as[43]

$$\dot{\mathbf{x}} = \mathbf{A}\mathbf{x} + \mathbf{B}\mathbf{u} + \mathbf{B}_2\mathbf{F}_b \tag{12}$$

On the left-hand side of Eq.(12) the state vector $\mathbf{x}$ contains the modal velocities $\dot{\mathbf{q}}$ and modal displacements $\mathbf{q}$ of the string and the soundboard, the velocity $\dot{y}_H$ and displacement of the hammer y_H, and can be written as $\mathbf{x} = (\dot{\mathbf{q}}, \dot{\mathbf{q}}_b, \mathbf{q}, \mathbf{q}_b, \dot{y}_H, y_H)^T$. This approach helps to produce a single state-space formulation that can be used for all the models that include the connection with a soundboard. For the reduced soundboard, there are 4 modal coordinates, and for the FE soundboard, 800. For the simplest soundboard representation, the K-V model with small added mass, only one modal coordinate is considered. The state-space matrix $\mathbf{A}$ can be defined as:

$$\mathbf{A} = \left[\begin{array}{cccc|cc} -\mathrm{diag}(2\zeta_n\omega_n) - \mathbf{C}_d & \mathbf{0} & -\mathrm{diag}(\omega_n^2) - \mathbf{K}_d & \mathbf{0} & \mathbf{0} & \mathbf{0} \\ \mathbf{0} & -\mathrm{diag}(2\zeta_{n_b}\omega_{n_b}) & \mathbf{0} & -\mathrm{diag}(\omega_{n_b}^2) & \mathbf{0} & \mathbf{0} \\ \mathbf{I}_{n\times n} & \mathbf{0}_{n\times n} & \mathbf{0}_{n\times n} & \mathbf{0}_{n\times n} & \mathbf{0} & \mathbf{0} \\ \mathbf{0}_{n_b\times n_b} & \mathbf{I}_{n_b\times n_b} & \mathbf{0}_{n_b\times n_b} & \mathbf{0}_{n_b\times n_b} & \mathbf{0} & \mathbf{0} \\ \hline \mathbf{0} & \mathbf{0} & \mathbf{0} & \mathbf{0} & 0 & 0 \\ \mathbf{0} & \mathbf{0} & \mathbf{0} & \mathbf{0} & 1 & 0 \end{array}\right] \quad (13)$$

For the different soundboard models, matrix **A** contains information about the damping ratio and natural frequencies of each string and soundboard mode within the correspondent modal damping and stiffness matrices. The damping ratio ζ_n should be that of the string disconnected from the soundboard; this is characterized below in section IV. To attenuate the vibration occurring in the damped segment of the string, a method consisting in coupling several dashpots has been used previously by Jiolat et al.[44]. In the present work, a distributed damper and spring is used to modify the modal damping and stiffness matrix respectively, embedded in the state-space matrix **A** in Eq.(12). They take the form:

$$\mathbf{C}_d = \int_{L_s}^{L_s+L_d} c_d \boldsymbol{\phi}_n(x)\boldsymbol{\phi}_n^T(x)dx \quad (14)$$

$$\mathbf{K}_d = \int_{L_s}^{L_s+L_d} k_d \boldsymbol{\phi}_n(x)\boldsymbol{\phi}_n^T(x)dx$$

where L_d is the length of the duplex scaling segment, c_d and k_d are the damping and stiffness coefficients that are defined (see below section V, E) to represent the strip of felt that usually mutes the duplex scaling segment in the mid-low register. The row vector $\boldsymbol{\phi}_n(x)$ corresponds to the mode shape function evaluated across L_d.

The matrix **B** in Eq.(12) can be written as:

$$\mathbf{B} = \begin{bmatrix} \boldsymbol{\phi}_e^T \\ \mathbf{0} \\ - \\ -1/m_H \\ 0 \end{bmatrix} \tag{15}$$

Matrix $\mathbf{B}$ is a column vector containing string mode shapes at the excitation point e, $\boldsymbol{\phi}_e^T$ as well as the inverse of the hammer mass. It is used to transform the force due to the hammer F_e into modal forces. The external force vector $\mathbf{u}$ is simply composed of F_e. The remaining modal force term $\mathbf{B_2F}_b$ is:

$$\mathbf{B_2F_b} = \begin{bmatrix} \boldsymbol{\phi}_s^T & \mathbf{0} \\ \mathbf{0} & \boldsymbol{\phi}_b^T \\ \mathbf{0} & \mathbf{0} \\ - & - \\ 0 & 0 \\ 0 & 0 \end{bmatrix} \begin{bmatrix} -F_b \\ F_b \end{bmatrix} \tag{16}$$

which introduces the modal contact force between the string and the soundboard. This term couples the soundboard and the string at their connection point using the string mode shapes $\boldsymbol{\phi}_s$, and the soundboard mode shapes $\boldsymbol{\phi}_b$ at the connection point b.

The physical displacements and velocities of the different parts of the system are calculated as

$$\mathbf{y} = \mathbf{Cx} \tag{17}$$

where the matrix $\mathbf{C}$ has the function of converting the modal coordinates to physical coordinates, and the output $\mathbf{y}$ contains the physical velocities and displacements of the string, the soundboard at the connection point and hammer; these are required to calculate the forces in Eq.(4) and Eq.(9) at each time step of the integration. Expanding, this equation takes the form:

$$\begin{bmatrix} \dot{y}_s \\ \dot{y}_b \\ y_s \\ y_b \\ \dot{y}_H \\ y_H \end{bmatrix} = \begin{bmatrix} \boldsymbol{\phi}_s & \mathbf{0} & \mathbf{0} & \mathbf{0} & 0 & 0 \\ \mathbf{0} & \boldsymbol{\phi}_b & \mathbf{0} & \mathbf{0} & 0 & 0 \\ \mathbf{0} & \mathbf{0} & \boldsymbol{\phi}_s & \mathbf{0} & 0 & 0 \\ \mathbf{0} & \mathbf{0} & \mathbf{0} & \boldsymbol{\phi}_b & 0 & 0 \\ 0 & 0 & 0 & 0 & 1 & 0 \\ 0 & 0 & 0 & 0 & 0 & 1 \end{bmatrix} \begin{bmatrix} \dot{\mathbf{q}} \\ \dot{\mathbf{q}}_b \\ \mathbf{q} \\ \mathbf{q}_b \\ \dot{y}_H \\ y_H \end{bmatrix} \tag{18}$$

The mode shapes $\boldsymbol{\phi}$ are obtained at the excitation point and at the connection point to obtain the relevant physical quantities. Evaluating the mode shapes at different positions and modifying $\mathbf{C}$ accordingly can give the vibration response of the string at any arbitrary position.

C. Simply supported string

In the case where the connection between the string and the soundboard is not included in the model, the string is considered as simply supported at its ends, with a total length equal to its speaking length L_s. Eq.(12) becomes:

$$\dot{\mathbf{x}} = \mathbf{A}\mathbf{x} + \mathbf{B}\mathbf{u} \tag{19}$$

where now the state space vector includes only the modal coordinates of the string and the physical velocities and displacements of the hammer $\mathbf{x} = (\dot{\mathbf{q}}, \mathbf{q}, \dot{y}_H, y_H)^T$. The state-space matrix $\mathbf{A}$ is now reduced to include only the modal damping and modal stiffness matrix of the string:

$$\mathbf{A} = \begin{bmatrix} -\mathrm{diag}(2\zeta_n\omega_n) & -\mathrm{diag}(\omega_n^2) & | & \mathbf{0} & \mathbf{0} \\ \mathbf{I}_{n\times n} & \mathbf{0}_{n\times n} & | & \mathbf{0} & \mathbf{0} \\ - & - & - & - & - \\ \mathbf{0} & \mathbf{0} & | & 0 & 0 \\ \mathbf{0} & \mathbf{0} & | & 1 & 0 \end{bmatrix} \tag{20}$$

The modal forcing term $\mathbf{B}\mathbf{u}$ remains unaltered.

D. Numerical integration

Numerical time integration is performed to obtain the time-dependent output vector from the state-space model, containing the velocities and displacements of the coupled system at the connection point. The time resolution of the response dt is defined as $dt = 1/f_s$ in terms of a required sample frequency f_s. This, in turn, is defined in terms of the maximum natural frequency analyzed and set to $f_s = 10f_{\max}$, where $f_{\max}$ is the highest natural frequency considered for the string. The initial conditions of the state-space vector $\mathbf{x}$ are:

$$\begin{gathered}\dot{\mathbf{q}}, \dot{\mathbf{q}}_b, \mathbf{q}, \mathbf{q}_b = \mathbf{0} \\ \dot{y}_H = 2.5\ \mathrm{m/s}, y_H = 0.05\ \mathrm{m}\end{gathered} \tag{21}$$

where initial conditions for the modal coordinates are applicable for both string and soundboard. The numerical time integration of the input state-space equation for the different cases, i.e., in Eq.(12) or Eq.(19), is performed in MATLAB using ode45, which is based on the fourth-order Runge-Kutta method.

IV. DAMPING OF A PIANO STRING

Although most of the string parameters are available in the literature, the model developed in this work requires the structural damping of the string disconnected from the bridge and tensioned between the agraffe and the hitch pin. This is generally not available and was therefore measured experimentally. To uncouple the string from the soundboard, two example strings were lifted using a metal cylinder placed near the hitch pin and fitted between the string and the cast-iron frame, as shown in Figure 7. The string was therefore lifted by 2-3 mm to avoid contact with the bridge. Measurements were also performed with the string coupled to the soundboard for comparison.

Figure 7. (color online) Cylinder used to lift string to decouple it from the soundboard.

Free vibration of the string was excited by means of a piano hammer and the vibration decay was analyzed to evaluate the damping. The transverse velocity response at a point close to the hammer striking position was recorded using a Laser Doppler Velocimeter.

Prior the calculation of the energy decay, the velocities where filtered in frequency bands of bandwidth $\Delta f = f_0$, where f_0 is the fundamental frequency; the bands were centered at the partials of the recorded tone. The energy decay in each band was calculated using the Schroeder integral as[45]:

$$E(t) = \int_t^{\infty} v_f^2(\tau) d\tau \tag{22}$$

where v_f represents the filtered measured velocity of the string in the direction perpendicular to the soundboard. Negligible double polarization was observed with this setup, whereas in the case of the string coupled to the soundboard, the energy associated with the decay will be influenced by the different polarizations of the string. The reverberation time T_{60} can be calculated by fitting a straight line to a manually chosen range of the energy decay curve in decibels to obtain the slope. Then the damping ratio ζ corresponding to a frequency band with central frequency f_c was found from[46]:

$$\zeta = \frac{1.1}{\mathrm{T}_{60} f_c} \tag{23}$$

Estimated values ζ for two uncoupled strings, a C2 (copper-wound) and F4 (steel) string, are shown as diamonds in Figure 8 and Figure 9. The estimated damping for the case where the strings are connected with the soundboard are also shown (circles). In the uncoupled strings, the results for F4 are more disperse than for C2, due to limitations of the measurement technique used to try to avoid the hammer hitting other unison strings, which in reality are not independent strings: they consist in a single string that is chorded through the hitch pin of the piano, as shown in the photo of the piano string configuration in Figure 10.

Thus, hitting other strings will result in undesired vibration in the measured string segment. These string segments were therefore lifted, which produced a change in tension, causing variable string frequencies. However, the resultant damping ratios did not vary significantly.

The measured damping ratios are compared for reference with the viscous damping model (SVM) as proposed by Chabassier[5;47;48] and used also more recently by Tan[49]. There is generally a good agreement between the measured values and the SVM, which is here implemented using the values available in the literature for this note and not by curve fitting it with this set of measurements. Although the results are slightly frequency dependent a constant value for ζ of all the modes could be also used as a reasonable approximation for the decoupled string. This was set to 5×10^{-5} for the copper-wound string and to 7.5×10^{-5} for the steel string (continuous lines in Figure 8 and Figure 9). In comparison to the structural damping of the string alone, the damping ratios of the string coupled to the soundboard are higher at low frequency by about a factor of 5-10 while they tend towards the damping ratios of the string alone at higher frequencies. It is to be expected that the model of the coupled string (see below) would be able to replicate this effect.

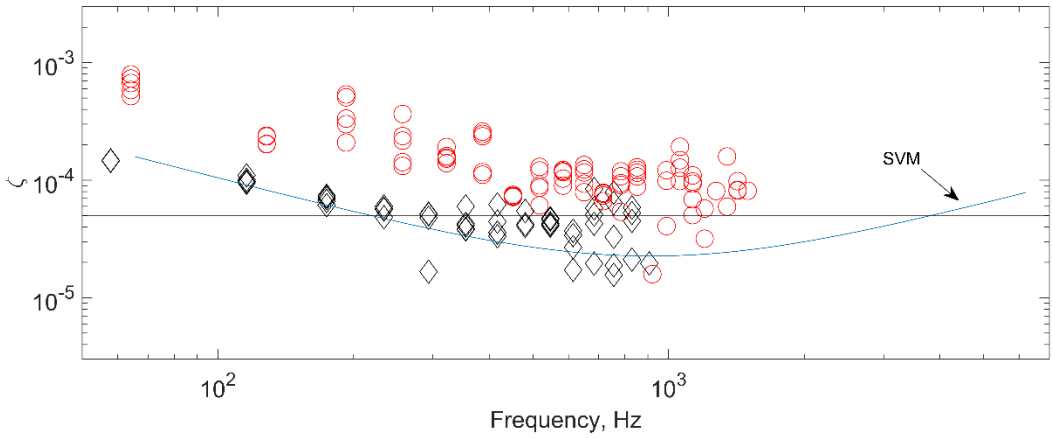

Figure 8. (color online) Estimated damping ratios ζ for C2 string. Circles (red) string coupled to the soundboard. Diamonds (black) decoupled string.

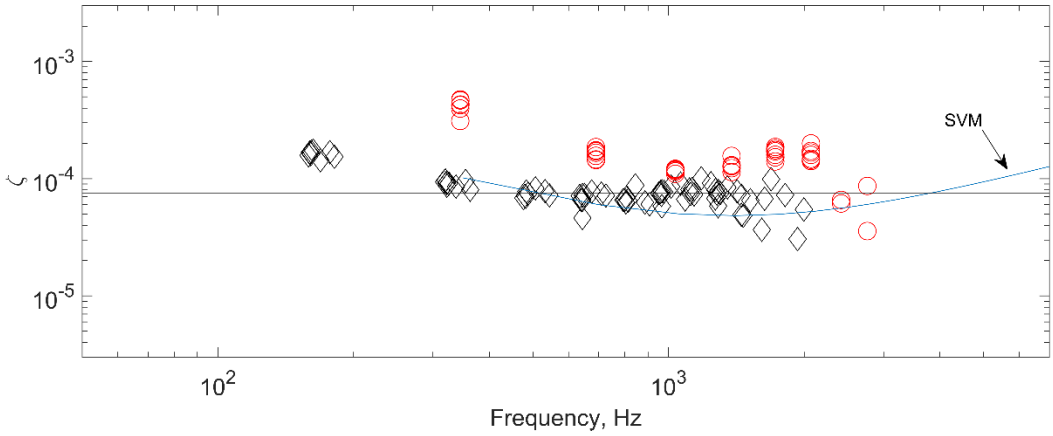

Figure 9. (color online) Estimated damping ratios ζ for F4 string. Circles (red) string coupled to the soundboard. Diamonds (black) decoupled string.

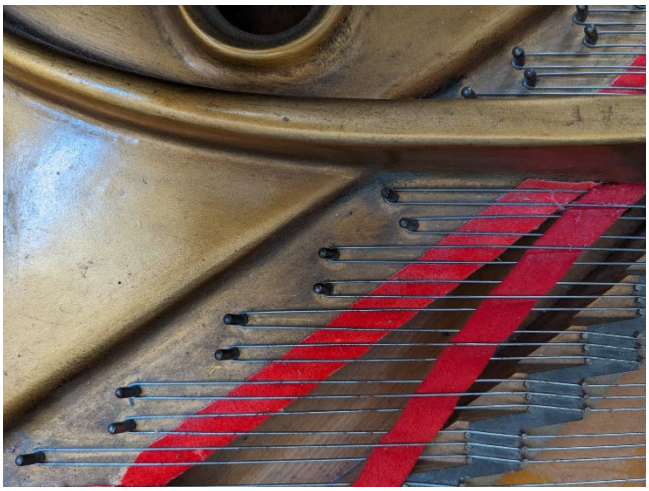

Figure 10. (color online) Piano string configuration in the middle-register of the piano.

V. TIME-DOMAIN MODEL RESULTS

Results from the time-domain model are shown here to illustrate the various physical phenomena occurring in the piano string vibration. The hammer-string contact force is shown as well as the subsequent string vibration at different locations. The interaction force between string and soundboard is also described, including the vibration response at a point on the soundboard. Comparisons are made using the different models described in section II-B and the simply supported string (II-C) used as a reference to emphasize the presence of additional damping added by the connection with the soundboard. Following this a minimal model is introduced, composed of a simply supported string with the damping adjusted to include that introduced by the connection with the soundboard. Finally, the influence of including a distributed damping and stiffness along the duplex scaling segment of a string is shown.

Three different notes across the piano range are considered for the analysis: A1, D4, and D5. For the different strings analyzed, the soundboard dynamics is that of the corresponding connection point. The parameters used for the strings are summarized in Table 3. Some of these were obtained from measurements on the available piano while others were obtained from literature, as indicated.

Table 3: String and hammer parameters

Description	Variable	Units	A1	D4	D5
Speaking length	L_s	m	1.3	0.59	0.308
Agraffe segment	L_e	m	1.56×10^{-1}	7.1×10^{-2}	3.4×10^{-3}
Duplex length	L_d	m	0.11	0.15	0.05
Tension	T	N	1821	637	1420
Young's modulus[41]	E	GPa	200	200	200
Density of string steel core[50]	ρ_c	$\mathrm{kg/m^3}$	7860	7860	7860
Density of copper winding[51]	ρ_w	$\mathrm{kg/m^3}$	8960	–	–
Diameter of steel string core	d_{core}	m	1×10^{-3}	1×10^{-3}	1×10^{-3}
Diameter of copper winding	d_{wound}	m	1.5×10^{-3}	–	–
Fundamental frequency of string	f_0	Hz	55	294	584
Piano hammer mass[48;52]	m_H	kg	10.4×10^{-3}	8.6×10^{-3}	7.8×10^{-3}

Piano hammer stiffness coefficient[48;52]	K_H	$\mathrm{N/m^p}$	2.15×10^8	7.45×10^9	3.23×10^{10}
Piano hammer nonlinear coefficient[48;52]	p	$-$	2.28	2.41	2.58

In Table 3, the steel core of the string and its copper winding, noted with the subscripts $core$ and $wound$ respectively, are used to obtain the corrected physical properties of the copper-wound string, in this case A1, as in Conklin[53]. The agraffe segment corresponds to the distance from the agraffe termination of the string to the point at which the hammer strikes. It is calculated using the relative striking position α given in Chaigne and Askenfelt[41], $L_e = \alpha \times L_s$, where α can take the values 0.12 for A1 and D4 , and 0.11 for D5.

For ease of comparison the time-domain results are shown for the first 5 s even when the decay lasts longer than this. Four different approaches are compared: (i) FE soundboard, (ii) reduced modal soundboard, (iii) Kelvin-Voigt soundboard and (iv) simply supported string (no soundboard). The influence of using different representations of the soundboard dynamics is discussed.

The results presented below initially include a duplex scaling segment left to vibrate, which highlights the capability of this modelling approach to include this feature that is adopted in most grand pianos in the mid-high register. At the same time, as discussed in section E, the inclusion of distributed damping and stiffness along the duplex scaling length is shown to be an effective modelling approach to mute the vibration of this segment of the strings in the mid-low register[1].

A. Hammer-string contact force

The hammer-string forces obtained with the four different models are generally not affected by the soundboard model. For note A1 the results in Figure 11 show that the forces do not vary when

using different soundboard representations. The results of the contact profile are similar to the ones produced by other modelling approaches taken in literature for C2[52]. The variations in the contact force for D5 are also negligible while for D4 the simply supported string results in a force that is different from the other models, whereas for the three models that include the soundboard the forces are identical (results not shown here).

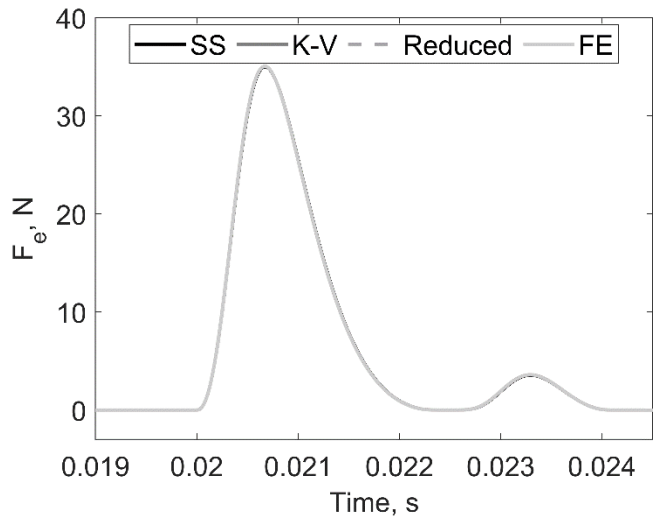

Figure 11. Hammer-string contact force for string A1.

B. String vibration and decay

To verify the effects of the different modelling approaches on the vibration velocity of the string in the time domain, the envelopes of the time histories are analyzed in this section and the damping ratios of the string-soundboard systems are also extracted.

The envelopes of the vibration velocity obtained at the excitation point are shown in Figure 12 for the three notes considered and the four different models. The vibration decays obtained with the simply supported string are longer than all the other models. This is due to the absence of the damping provided by the connection with the soundboard, the only damping mechanism being the structural damping estimated in Section IV. The other three models provide similar results. For A1

and D5 some differences occur at the beginning of the response where the reduced soundboard model is closer to the full FE representation than the Kelvin-Voigt model.

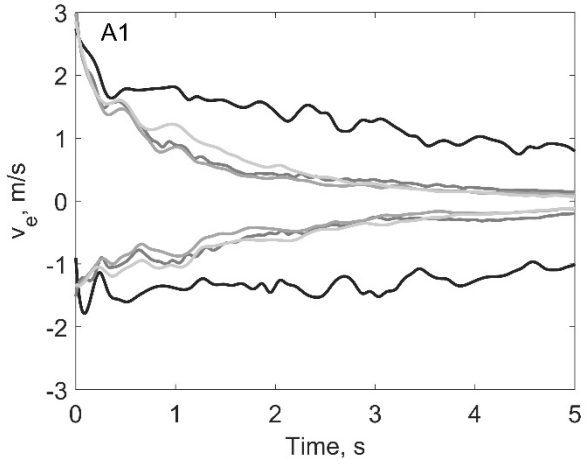

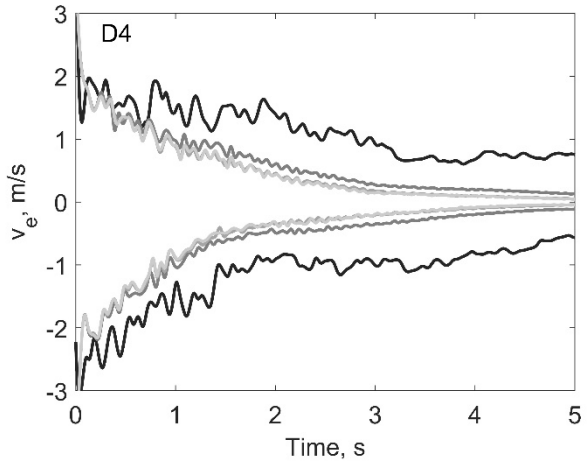

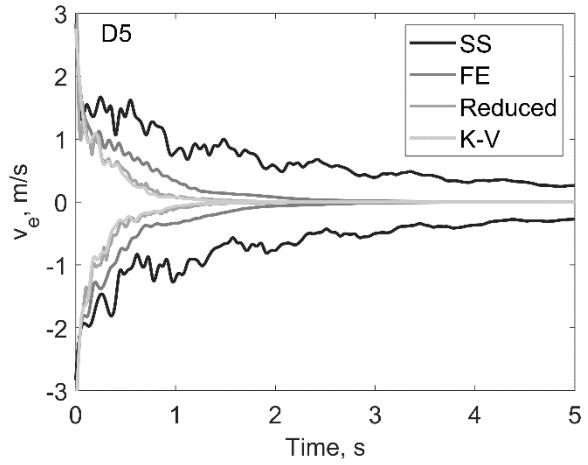

Figure 12. Envelopes of time histories of piano string vibration velocity at the excitation point.

To quantify the differences seen in Figure 12 and evaluate the modelling approaches, it is of interest to calculate the damping introduced by the connection with the soundboard numerically and compare it with the experimental results shown in Figure 8 and Figure 9. The comparisons are presented in Figure 13 for the A1 string, where the damping estimations from both measurements and numerical models are obtained using the same procedure, described in section IV.

The damping of the simply supported case corresponds to the constant structural damping ratio estimated from measurements, while the other models follow the trend of the measurements performed with the string connected to the soundboard. The reduced modal representation gives results closest to the FE soundboard model, particularly at lower frequencies below 600 Hz. At high frequencies the estimated damping of the coupled models tends to that of the simply supported string. Similar conclusions hold for the other strings analyzed but the results are not presented here for brevity.

It can be seen that the damping ratios exhibit a squence of dips. Although they are not clearly identifiable in the measurements, the dips in the modal soundboard results align with the duplex scaling resonances. This is because damping estimates for frequencies at and close to the resonance of the duplex scaling segment are affected by vibration transmission beyond the bridge and into this segment. This is a typical characteristic of piano string vibration since it was patented by Steinway[54;55] and a feature of the model, and its effect on the estimated damping ratio is therefore considered.

Although the general trend of the damping ratios is satisfactory in comparison with the measurements, some differences occur. These can be explained by the limitations and assumptions of the current models. The differences below 100 Hz, where the damping from the measurements is higher than the models, could be associated with differences between experimental and model mobilities. These differences have less influence at higher frequencies, but here double polarization

may have a significant effect. Double polarization can produce a two-stage decay, hence smaller apparent damping. An experimental method for estimating the damping of the two transverse directions of vibration of a uncoupled string were shown by Tan[49]. Nonetheless, assumes that strings have a non-linear behaviour and imperfections in the excitation that can excite the direction parallel to the soundboard. Herein, the model is assumed to be linear, the hammer excitation is perfectly transverse and the response in the second polarization is caused only by the connection with soundboard. Tan's experimental results were processed using high resolution modal analysis techniques consisting in the separation of the signal into sinuosids with a corresponding decay, phase, and natural frequency[56;57].

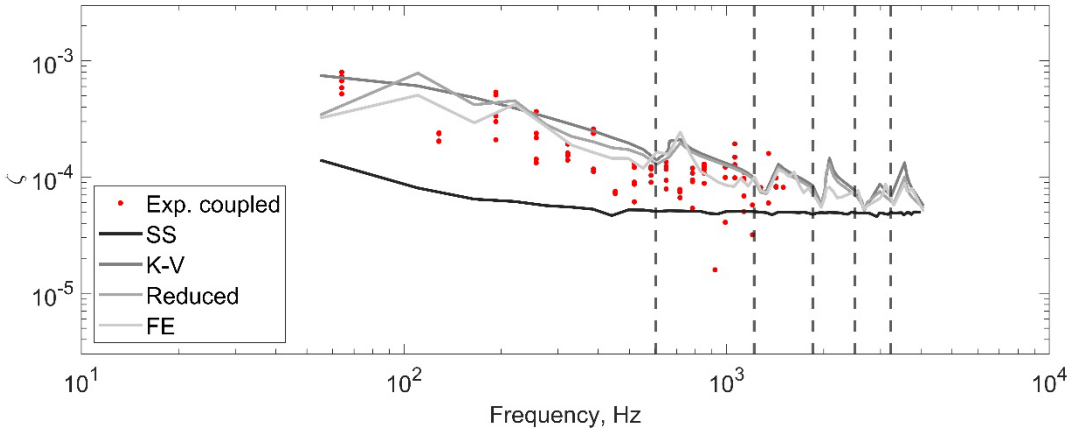

Figure 13. (color online) Damping ratios for A1 string connected to the soundboard, estimated from modelling and experiments. Vertical dashed lines indicate resonances of the duplex scaling segment.

To conclude the assessment of string vibration, the spectra of vibration velocity at the excitation point and the connection point with the bridge are shown in Figure 14 for the A1 string by way of example. The simply supported model is included for reference only, and is fixed at the connection point and hence this model is not present in Figure 14(b). The main feature of the spectra is the familiar series of partials for this note. At the excitation point in Figure 14(a) there is no identifiable presence of the soundboard resonances but the frequencies associated with the duplex scaling

segment can be identified by small peaks at 660 Hz and its higher harmonics, indicated in the figure. At the bridge connection point shown in Figure 14(b), two low-frequency soundboard resonances are present for the two models that include them. Other resonances occurs close to the fundamental frequency of this note and is therefore not separately identifiable. The duplex scaling frequencies are also present and more distinct than at the hammer striking point.

Considering the three models that include a connection with the soundboard, the string partials have similar levels. However, more similiarities exist between the two modal soundboard models. An example is highlighted in Figure 14(b), where at the first string partial the K-V model has a lower level than the other two models. A higher resonance is also highlighted showing that the differences are smaller than at lower frequencies. This is caused by differences in the mobility of the soundboard (see Figure 6) at lower frequencies, where it is comparable to that of the contact stiffness, whereas at higher frequencies the contact spring mobility is higher than that of the soundboard, and the soundboard has negligible influence on the string vibration. This shows that the higher frequency range, in which the simpler soundboard representations are less accurate (see Figure 5), is dominated by the interaction between the string and the contact stiffness, whereas the soundboard representation has a diminished role. For D4 or D5, where the string partials are higher in frequency, the interaction is dominated by the contact stiffness as its mobility is comparable or higher than that of the soundboard.

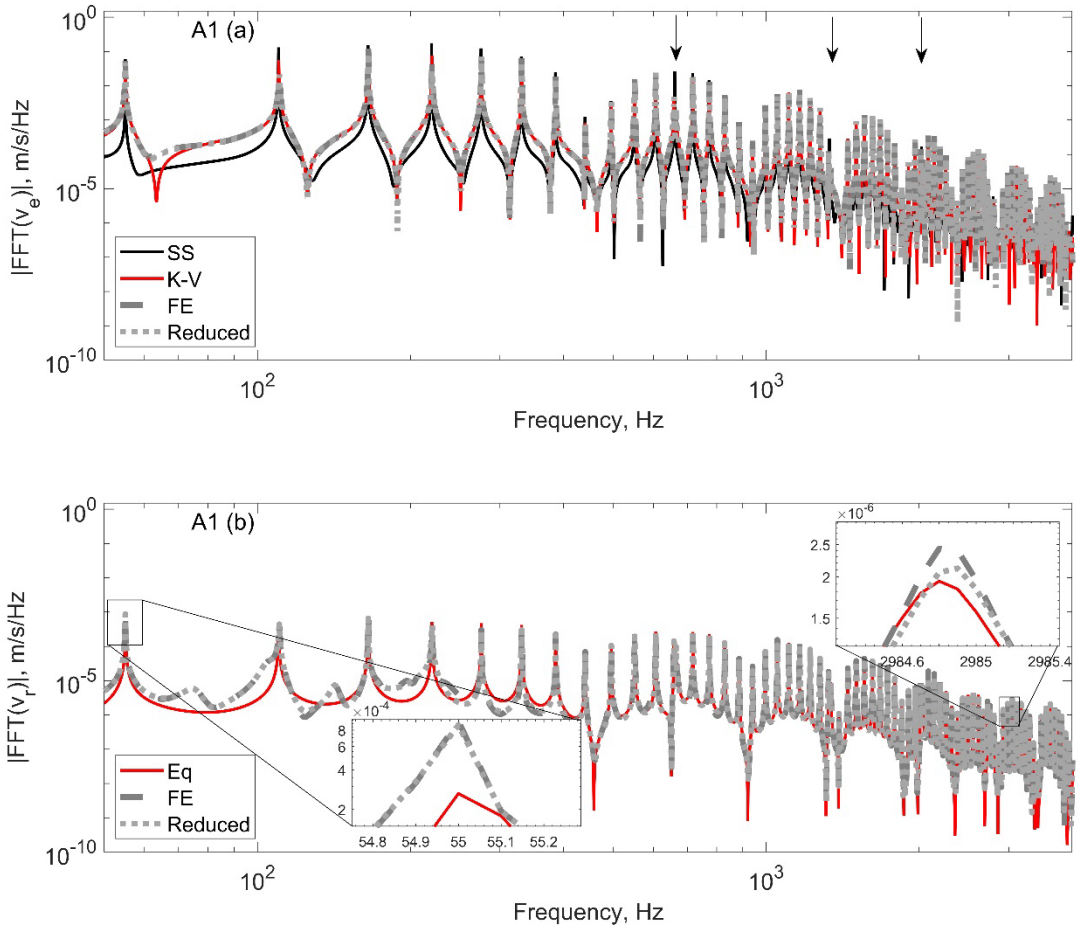

Figure 14. (color online) Spectra of vibration velocity for note A1: (a) at the excitation point, duplex scaling resonances are indicated by the arrows, and (b) at the connection point.

Although the soundboard models produce similar results, the computational times required differ significantly. For the D4 case, on a standard desktop computer and with the ode45 Matlab routine the computational time required to calculate 10 s of time history with a sampling frequency of $f_S \sim 63$ kHz are as follows. The reduced representation requires about 37 s, the K-V takes 54 s and the FE representation requires approximately 840 s. The K-V model requires more computational time than the more complex reduced model because the former includes high damping. This hypothesis was tested by running the K-V under different damping coefficients, showing that computational time can be reduced as much as to 25 s when reducing damping by orders of

magnitude. The computational time are also related to the ode45 solver adopted in study and can vary with the numerical implementation.

C. Force at the bridge and soundboard response

In the interaction between the string and the soundboard, it is of interest to compute the interaction force between the two systems. This force is the responsible for the coupling and it can be used as an input for obtaining the vibratory response of the soundboard. In the case of the simply supported string, in absence of the soundboard, the force is given by Eq.(3). Once computed, the forces from the different models can be used for sound generation in future work.

The envelopes of the time histories of the forces at the bridge are shown in Figure 15. The general trend of these results confirms that lower tones last longer and result in higher values of the force. Comparing the different soundboard models, the simply supported approach produces decays that are much longer than the others, as found for the string vibration. Although the reduced soundboard model is closer to the FE representation, the differences in terms of transmitted force are more subtle than for the string vibration. The largest difference is for D5 where the response is larger in the FE model. The time histories of the force decay do not seem to favour a particular representation of the soundboard. The readers can make their own subjective judgement from the audio files Mm. 1, Mm. 2, Mm. 3 and Mm. 4 for the A1 model, and Mm. 5, Mm. 6, Mm. 7 and Mm. 8 for the D4 model.

Mm. 1. Transmitted force to the soundboard F_b, for A1, simply supported string.

Mm. 2. Transmitted force to the soundboard F_b, for A1, FE soundboard model.

Mm. 3. Transmitted force to the soundboard F_b, for A1, reduced soundboard model.

Mm. 4. Transmitted force to the soundboard F_b, for A1, K-V soundboard model.

Mm. 5. Transmitted force to the soundboard F_b, for D4, simply supported string.

Mm. 6. Transmitted force to the soundboard F_b, for D4, FE soundboard model.

Mm. 7. Transmitted force to the soundboard F_b, for D4, reduced soundboard model.

Mm. 8. Transmitted force to the soundboard F_b, for D4, K-V soundboard model.

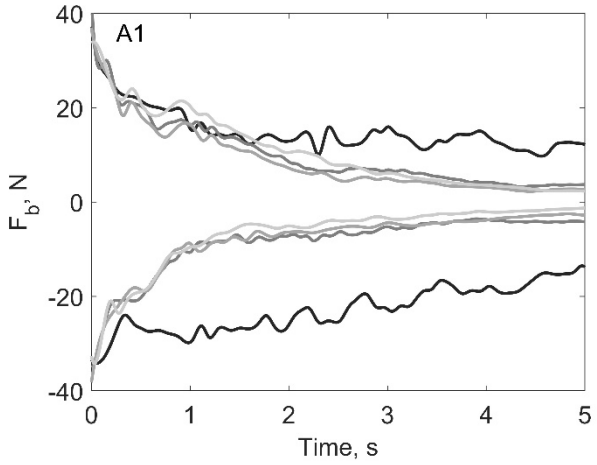

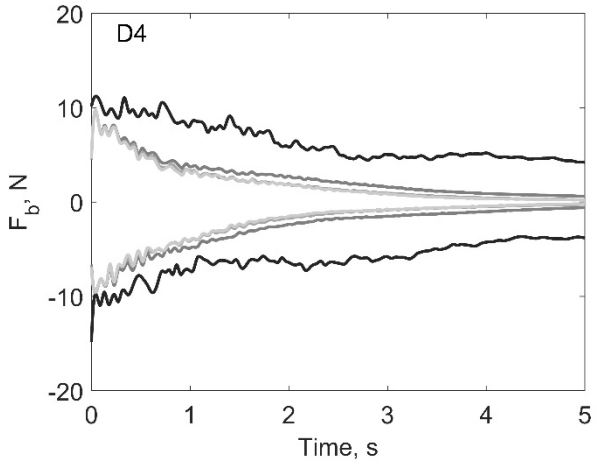

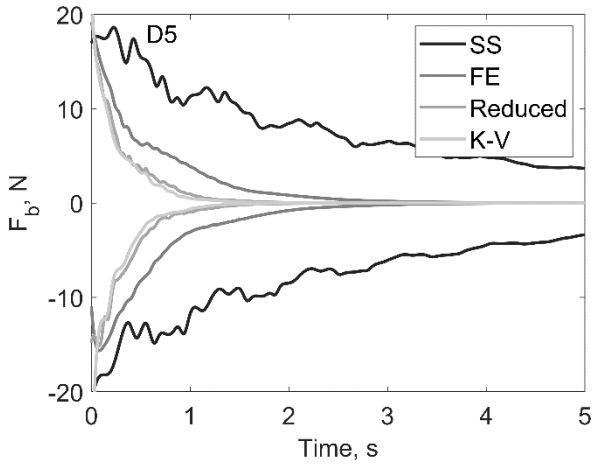

Figure 15. Envelopes of time histories of force transmitted to the soundboard.

The force spectra of the different representations are shown in Figure 16. The simply supported case is omitted for ease of comparisons between the other models. There is no sign of soundboard resonances in the force spectra in contrast to what is seen in the string vibration at the connection point (see Figure 14(b)). The duplex scaling resonances are present in the transmitted force at 660 Hz for the A1 string, and 1110 Hz for D4, as well as their higher harmonics. For D5 only one resonance is present at 3.8 kHz.

Generally, the models that include the dynamics of the soundboard have similar peaks in their force spectra, both in level and in frequency, while the K-V model has peaks that are slightly different in magnitude and frequency, see for instance the highlighted first peak for A1. The case of D4 shows that the differences are consistent through the frequency range. At this location there exists a greater impedance mismatch between the string and soundboard than in the other locations on the bridge. Consequently, the soundboard model does not influence the results significantly and the interaction with the contact stiffness is predominant. Although the differences are generally small, the reduced model is closer to the FE model than the K-V model.

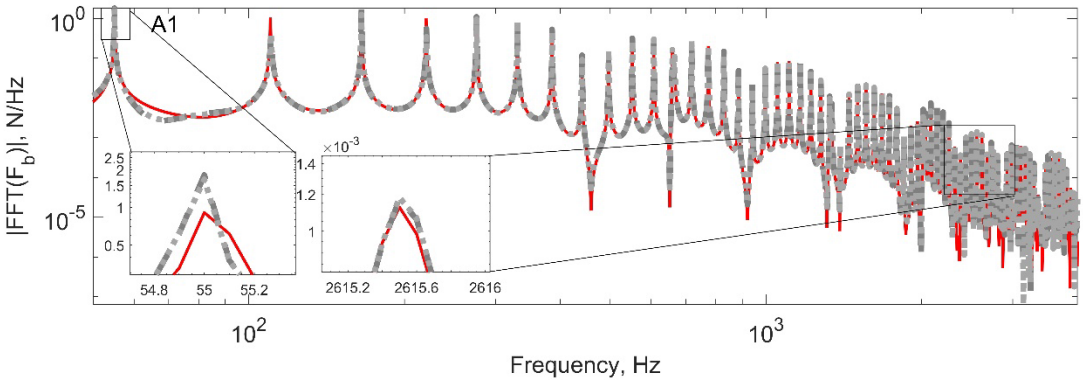

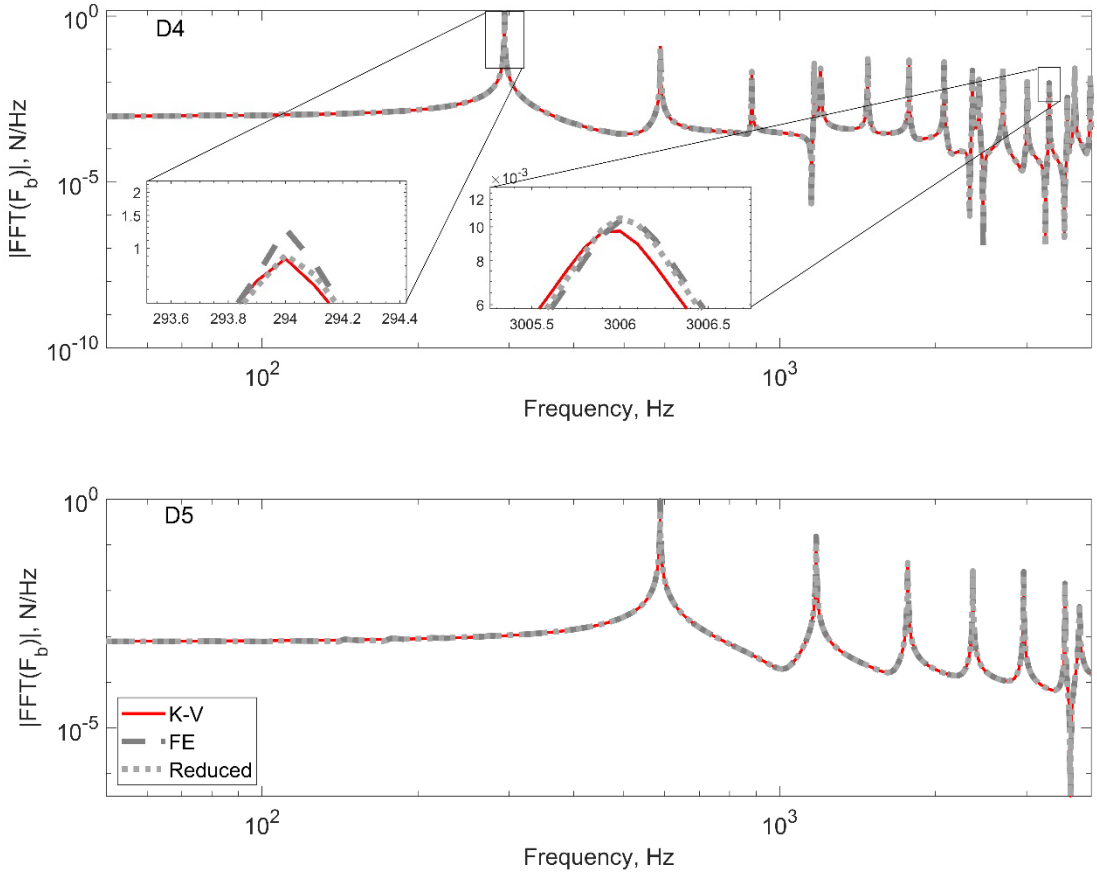

Figure 16. (color online) Spectra of force transmitted to the soundboard.

The forces at the bridge can then be used to evaluate the vibration response at any point on the soundboard by combining them with the impulse response between the bridge, point b (see Figure 1), and a generic point k on the soundboard shown in Figure 3. The transfer impulse responses are obtained by calculating the inverse Fourier transform of the transfer mobilities Y_{kb} evaluated with the full FE model (irrespective of which soundboard model is used in calculating the string vibration). Mathematically, the vibration velocity at k, caused by a bridge force F_b is the convolution between the bridge force and the impulse response as:

$$v_k(t) = IFFT(Y_{kb}) * F_b(t) \tag{24}$$

The envelopes of the time histories of the soundboard vibration are shown in Figure 17 for excitation of strings A1 and D4. These allow two cases to be compared in which the soundboard representation has a different importance. Whereas for the transmitted force in Figure 15, the soundboard models did not exhibit notable differences, the response of the soundboard using the K-V model has more noticeable differences particularly in the case of A1, where the soundboard model plays a more significant role. Compared with the forces shown in Figure 15, the profiles of the resultant velocity v_k are more regular and, moreover, the soundboard appears to enhance the differences between the K-V model and the modal soundboard models in the case where its mobility plays a more important role.

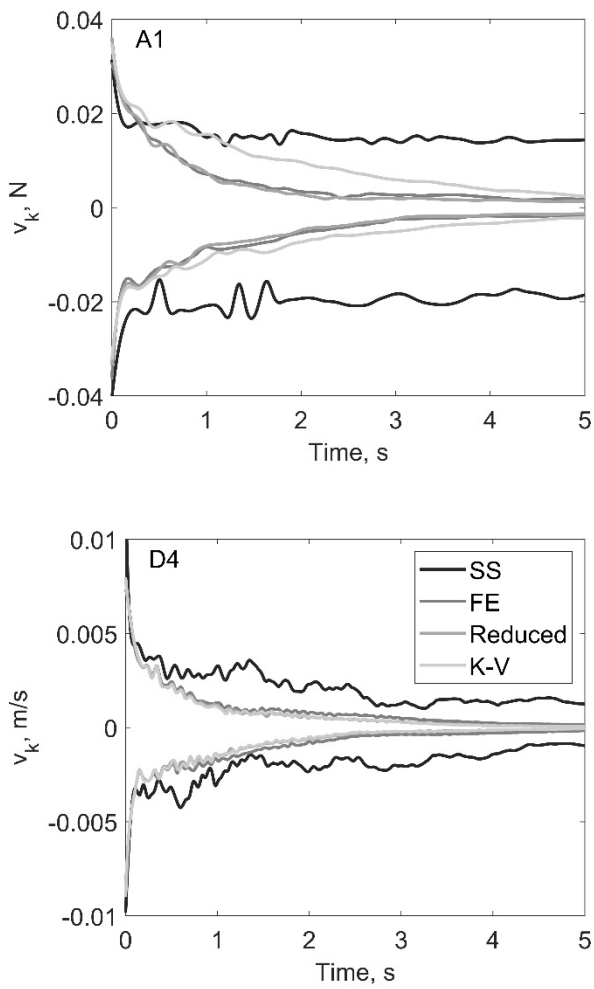

Figure 17: Vibration velocity envelope at a position on the soundboard

The spectra of the vibration of the soundboard are shown in Figure 18. The modes of the soundboard are now present in the vibration response for all the models due to the use of the same transfer mobility Y_{kb} in each case. Two example string partials are highlighted, showing that, as in the transmitted force, the models with soundboard dynamics produce similar resonances while those of the K-V model are slightly different. As was stated in other comparisons, the differences are more significant at lower frequencies, where the soundboard has a more significant influence.

The sound samples for the vibration velocity obtained via the reduced model for A1 and D4 are attached as Mm. 9 and Mm. 10. The listener should notice the influence of the soundboard. As the spectra are now richer in lower frequencies than the force sound samples, the sound is now "fuller". The simply supported model, not shown, gives a spectrum which reproduces adequately the main features obtained with the other approaches, but its decay is larger and unrealistic. It cannot include the duplex scaling resonances, but the damping value could be adjusted to represent the effect of the soundboard in an equivalent way. This is presented in the next section.

Mm. 9. Vibration velocity at the soundboard v_k, for A1, reduced soundboard model.

Mm. 10. Vibration velocity at the soundboard v_k, for D4, reduced soundboard model.

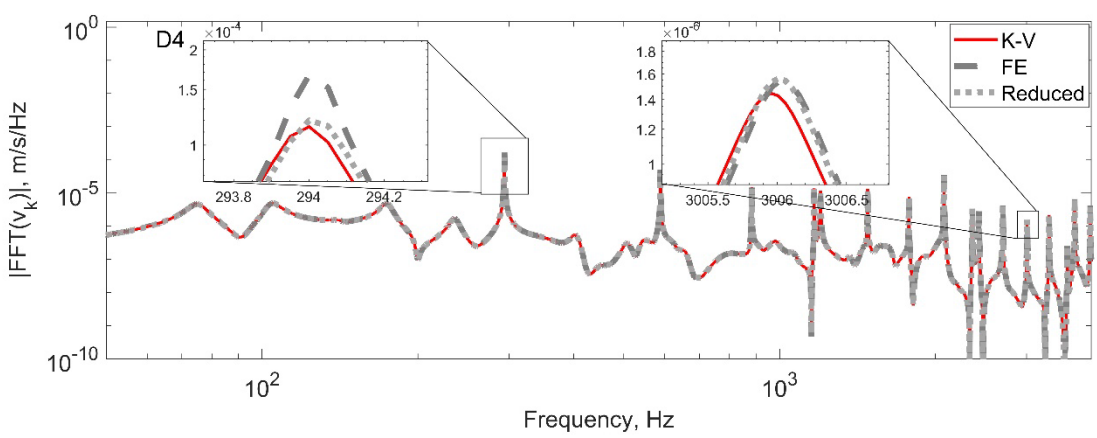

Figure 18. (color online) Spectra of vibration velocity at the soundboard.

D. A minimal model

The simply supported string model is modified to include the damping arising from the connection with the soundboard, which would yield shorter computational times while maintaining the characteristics of the piano tone due to the coupling between the string and the soundboard. The formulation of the minimal model is the one already presented in section III-C, but in this case the modal damping matrix is modified to include the estimated damping rations of the string coupled to the FE soundboard. The real part of the mobility is not used in this case. To test this, the estimated damping ratios of the string coupled to the FE soundboard model, shown in Figure 13, are used as an input to the modal damping matrix of a simply supported A1 string. The envelope of the string vibration velocity at the excitation point is compared in Figure 19 with that obtained from the string coupled with the FE soundboard model. The agreement between the two models is satisfactory and some differences in the envelopes can be attributed to uncertainty in estimating low values of damping ratios.

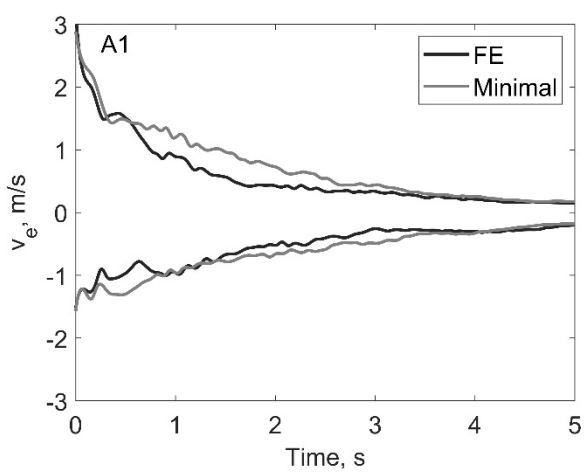

Figure 19. Time histories of piano string vibration velocity at excitation point for A1 string. Black line: string coupled with FE soundboard model. Gray line: simply supported string with adjusted damping ratio.

The comparisons are also made in the frequency domain: the spectra of the vibration velocity and the force transmitted to the soundboard are shown in Figure 20. The spectra have good agreement, but this minimal model fails to represent the vibration of the duplex scaling segment, which can be seen in the force spectrum in Figure 20(b), at approximately 660 Hz and higher harmonics.

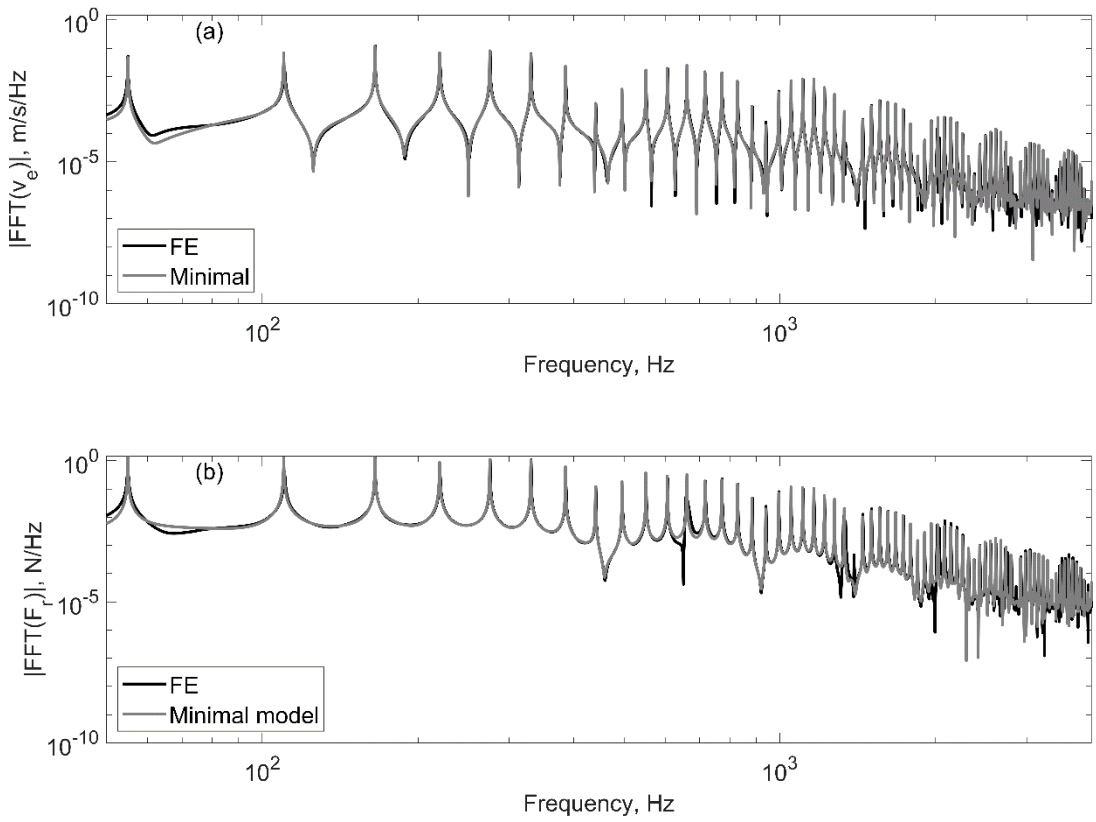

Figure 20. Comparisons of spectra between FE and minimal model for the A1 case. (a): Spectrum of vibration velocity at excitation point. (b): Spectrum of force transmitted to the soundboard.

E. Attenuating the duplex scaling segment

It has been shown in the previous sections that one of the features of the models that include the soundboard is the presence of resonances of the duplex scaling segment. However, in actual pianos these are muted in the lower register. The same models can still be adopted provided a suitable value for the distributed dampers and springs is applied in the duplex scaling segment. Using Eq.(14), different values of damping coefficients c_d in a range between 1 and $4\ \mathrm{Ns/m^2}$ are used to

determine what value can be used to obtain the desired effect without significantly affecting the other string resonances. The value of the distributed spring was fixed. The results are shown in Figure 21 for the spectra of the acceleration at the connection point of the soundboard b for the note D4 using a reduced soundboard model. Again, the readers can compare the different outcomes by listening to the audio files provided, Mm. 11, Mm. 12, Mm. 13 and Mm. 14 for increasing values of c_d. The stiffness by itself can provide a sufficient attenuation of the first resonance of the duplex scaling. Within the range of values tested, a value of $c_d = 1\ \mathrm{Ns/m^2}$ reduces the higher duplex scaling resonances in the numerical model adequately: the effect on the adjacent string resonances is smaller than when using higher values of c_d. This is shown in the highlighted resonance in Figure 21 a). For comparison, the measurement of acceleration at the bridge pin at the D4 location is shown, evidencing the lack of duplex scaling vibration in this piano. The modelled result has a satisfactory agreement with the measurement and confirms that the model approach taken and its coupling with the string is correct.

Mm. 11. Acceleration at the connection point of the soundboard a_b, for D4, using $c_d = 0\ \mathrm{Ns/m^2}$.

Mm. 12. Acceleration at the connection point of the soundboard a_b, for D4, using $c_d = 1\ \mathrm{Ns/m^2}$.

Mm. 13. Acceleration at the connection point of the soundboard a_b, for D4, using $c_d = 2\ \mathrm{Ns/m^2}$.

Mm. 14. Acceleration at the connection point of the soundboard a_b, for D4, using $c_d = 4\ \mathrm{Ns/m^2}$.

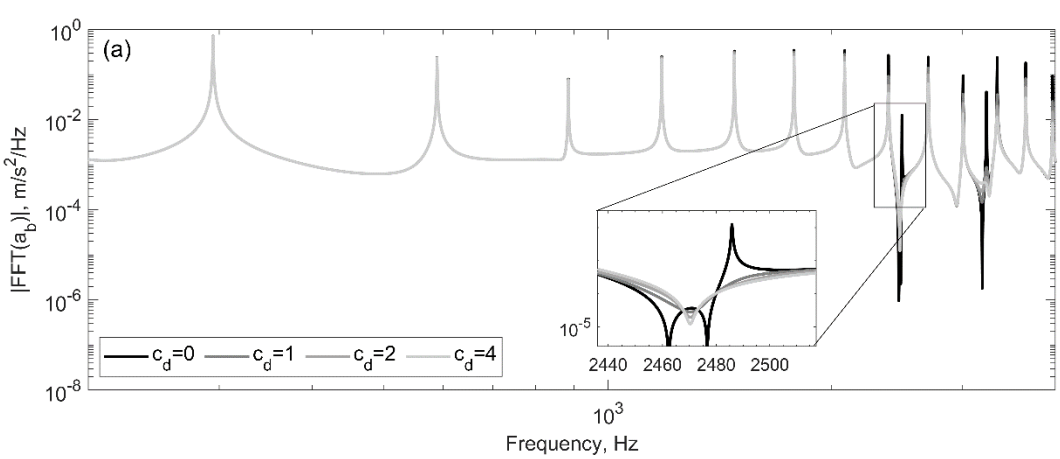

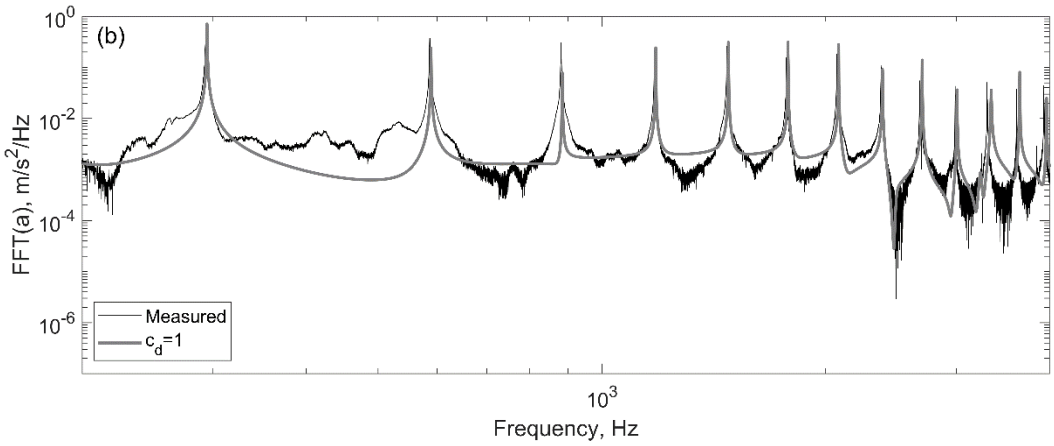

Figure 21. (a): Spectrum of acceleration at the connection point of the soundboard for D4 string, using different damping coefficients for the duplex scaling segment. (b): Spectrum of comparison between measured acceleration and modelled using highly damped duplex scaling.

VI. CONCLUSIONS

Soundboard models of differing complexity, a detailed FE model, a reduced modal model and a simplified Kelvin-Voigt model, have been coupled to a string in a state-space approach. The scope is to address the effects of the assumptions in using different soundboard models differing in complexity in their modal representation. Nonetheless, it is not intended to produce complex soundboard model accounting for nonlinear effects due to prestresses or other effects of its manufacturing. Moreover, the modelling approaches presented in this study assume a linear behaviour of the different systems associated to piano sound generation, with the exception of the hammer excitation.

The assumptions related to the soundboard have only a small effect on the results for the string response, affecting the lower frequency range more than higher frequencies. This is explained by the differences between mobilities of the string, the soundboard, and the contact spring used for the coupling between them. At lower frequencies the mobility levels of the soundboard are similar to those of the contact spring. Consequently, the string and soundboard can interact, and the

soundboard resonances have an influence on the resultant string vibration in this frequency range. On the other hand, at higher frequencies the contact spring mobility is much greater than that of the soundboard. Hence the response of the system is dependent on the interaction between the string and the contact spring, and the soundboard model does not significantly influence the results in this part of the spectrum. These observations are applicable at widely different locations in the piano range, for string vibration, interaction force between string and soundboard, and for the resultant vibration of the soundboard.

In contrast, the damping estimation is affected by the soundboard representation to some extent. The trend of the damping ratios shows irregularities that can be attributable to the presence of the duplex scaling vibrations in the models. Differences between the experimental results and the models at low frequencies may be caused by deviations between the experimental and modelled soundboard mobilities at the connection point. Another cause of differences could be the presence of double polarization in the experimental measurements, producing a longer decay and hence smaller damping. Double polarization is not yet included in the numerical models.

To provide a minimal model, a simply supported string model was modified to include the damping corresponding to that provided by the connection with the soundboard, yielding similar levels and spectra as a string connected with an FE soundboard model. However, this simply supported model does not include the duplex scaling segment resonances. Such a model could therefore be useful in low-mid range of the piano where this segment is muted.

Finally, a brief study on the attenuation of the duplex scaling segment shows that a small damping coefficient is needed to accomplish the desired effect, so as not to affect greatly other adjacent resonances. This was achieved by using a distributed damping and stiffness approach along the duplex scaling segment. Results were compared with measurements showing a satisfactory

agreement. However, it is yet to be confirmed experimentally what is the damping introduced by the felt in the duplex scaling.

Overall, it is clear that detailed FE soundboard models are not needed to represent the main characteristics of string-soundboard interaction. Simpler soundboard representations can achieve the expected results and can model the trend of the damping with less computational effort. The reduced model is more similar to the FE soundboard model than the K-V model, particularly at low frequencies, where the soundboard can influence vibration. Nonetheless, the K-V soundboard model is not far from representing the FE soundboard behavior. For a full 3D representation of strings and soundboard, a model considering a reduced modal soundboard would need to be extended to include different directions, and to consider other coupling mechanisms such as the interaction between unison strings. The force generated by these string-soundboard models could then be used to predict the vibration response across the soundboard, and hence the radiated sound, by applying the interaction force to a suitably complete model of the soundboard. To give an initial estimate of soundboard vibration, the velocity was obtained at a point on the soundboard, from which it can be heard from the corresponding audio files and seen how important the soundboard resonances are in the generated tone, producing a response that is enriched at lower frequencies.

ACKNOWLEDGMENTS

The authors are grateful to Prof. David O. Norris for facilitating access to the piano and Cesar Hernandez for the information about the soundboard. The first author is funded by the National Agency for Research and Development (ANID)/Scholarship Program/ DOCTORADO BECAS CHILE/2020 – 72210046.

AUTHOR DECLARATIONS

Conflict of Interest

The authors have no conflicts to disclose.

DATA AVAILABILITY

The data that support the findings of this study are openly available in [repository name] at http://doi.org/[doi], reference number [reference number].

REFERENCES

[1]F. Oberg, and A. Askenfelt. "Acoustical and perceptual influence of duplex stringing in grand pianos," J. Acoust. Soc. Am. **131**, 856-871 (2012)

[2]G. Weinreich. "Coupled piano strings," J. Acoust. Soc. Am. **62**, 1474 - 1484 (1977)

[3]B. Bank, and L. Sujbert. "A piano model including longitudinal string vibrations," in *Proceedings of International Conference on Digital Audio Effects (DAFx '04)*, Naples, Italy 2004).

[4]N. Giordano, and M. Jiang. "Physical modeling of the piano," EURASIP Journal on Applied Signal Processing **7**, 926–933 (2004)

[5]J. Chabassier, A. Chaigne, and P. Joly. "Modeling and simulation of a grand piano," J. Acoust. Soc. Am. **134**, 648 - 665 (2013)

[6]B. Elie, B. Cotte, and X. Boutillon. "Physically-based sound synthesis software for Computer-Aided-Design of piano soundboards," Acta Acustica **6** (2022)

[7]A. Chaigne, and A. Askenfelt. "Numerical simulations of piano strings. I. A physical model for a struck string using finite difference methods," J. Acoust. Soc. Am. **95** (1994)

[8]N. Giordano. "The physics of vibrating strings," Computers in Physics **12**, 138-145 (1998)

[9]J. Bensa, S. Bilbao, R. Kronland-Martinet, and J. O. Smith III. "The simulation of piano string vibration: From physical models to finite difference schemes and digital waveguides," J. Acoust. Soc. Am. **114**, 1095-1107 (2003)

[10]F. Pfeifle. "Real-time physical model of a piano-hammer string interaction coupled to a soundboard," in *Proceedings of International Symposium on Musical Acoustics*, Le Mans, France (July 7-12, 2014).

[11]C. Issanchou, S. Bilbao, J. L. L. Carrou, C. Touze, and O. Doare. "A modal-based approach to the nonlinear vibratin of strings against a unilateral obstacle: Simulations and experiments in the pointwise case," J. Sound Vib. **393**, 229-251 (2017)

[12]P. M. Valiente, G. Squicciarini, and D. J. Thompson. "Piano string vibration modelling using coupled mobilities and a state-space approach," in *Proceedings of Internoise 2022*, Glasgow, UK (August 21 -24, 2022).

[13]P. M. Valiente, G. Squicciarini, and D. J. Thompson. "Modeling the interaction between piano strings and the soundboard," in *Proceedings of Fourth Vienna Talk on Music Acoustics*, Vienna, Austria (September 11-14, 2022).

[14]G. Derveaux, A. Chaigne, P. Joly, and E. Becache. "Time-domain sumulation of a guitar: Model and method," J. Acoust. Soc. Am. **114**, 3368-3383 (2003)

[15]O. Inacio, J. Antunes, and M. C. M. Wright. "Computational modelling of string-body interaction for the violin family and simulation of wolf notes," J. Sound Vib. **310**, 260-286 (2008)

[16]V. Debut, J. Antunes, M. Marques, and M. Carvalho. "Physics-based modeling techniques of a twelve-string Portuguese guitar: A non-linear time-domain computational approach for the multiple-strings/bridge/soundboard coupled dynamics," Appl. Acoust. **108**, 3–18 (2016)

[17]J. T. Jiolat, C. d'Alessandro, and J.-L. L. Carrou. "Toward a physical model of the clavichord," J. Acoust. Soc. Am. **150**, 2350-2363 (2021)

[18]L. Trautmann, S. Petrausch, and M. Bauer. "Simulations of string vibrations with boundary conditions of third kind using the functional transformation method," J. Acoust. Soc. Am. **118**, 1763 - 1775 (2005)

[19]B. Bank, and L. Sujbert. "Generation of longitudinal vibrations in piano strings: From physics to sound synthesis," J. Acoust. Soc. Am. **117**, 2268 - 2278 (2005)

[20]A. M.-. Mani, J. Frelat, and C. Besnainou. "Numerical simulation of a piano soundboard under downbearing," J. Acoust. Soc. Am. **123**, 2401 - 2406 (2008)

[21]G. Squicciarini. "Vibroacoustic Investigation of a Grand Piano Soundboard," PhD dissertation, Politecnico di Milano, Milan,2012.

[22]A. Chaigne, B. Cotte, and R. Viggiano. "Dynamical properties of piano soundboards," J. Acoust. Soc. Am. **133**, 2456 - 2466 (2013)

[23]A. Askenfelt. "The strings and the soundboard," in *Five Lectures on the Acoustics of the Piano* (Stockholm, Sweden, 1990).

[24]K. Ege, X. Boutillon, and M. Rebillat. "Vibroacoustics of the piano soundboard: (Non)linearity and modal properties in the low- and mid-frequency ranges," J. Sound Vib. **332**, 1288-1305 (2013)

[25]R. Corradi, S. Miccoli, G. Squicciarini, and P. Fazioli. "Modal analysis of a grand piano soundboard at successive manufacturing stages," Appl. Acoust. **125**, 113-127 (2017)

[26]H. Suzuki. "Vibration and sound radiation of a piano soundboard," J. Acoust. Soc. Am. **80**, 1573 - 1582 (1986)

[27]J. Berthaut, M. N. Ichchou, and L. Jezequel. "Piano soundboard: structural behavior, numerical and experimental study in the modal range," Appl. Acoust. **64**, 1113-1136 (2003)

[28]B. Trevisan, K. Ege, and B. Laulagnet. "A modal approach to piano soundboard vibroacoustic behavior," J. Acoust. Soc. Am. **141**, 690-709 (2017)

[29]X. Boutillon, and K. Ege. "Vibroacoustics of the piano soundboard: Reduced models, mobility synthesis, and acoustical radiation regime," J. Sound Vib. **332**, 4261 - 4279 (2013)

[30]N. Fletcher, and T. Rossing. "Vibrations of a Stiff String," in *The Physics of Musical Instruments* (Springer, NY, USA, 1998).

[31]D. J. Ewins. *Modal Testing: Theory, Practice and Application* (Wiley), 2003.

[32]B. Elie, F. Gautier, and B. David. "Macro parameters describing the mechanical behavior of classical guitars," J. Acoust. Soc. Am. **132**, 4013-4024 (2012)

[33]E. Skudrzyk. "The mean-value method of predicting the dynamic response of complex vibrators," J. Acoust. Soc. Am. **4**, 1105-1135 (1980)

[34]A. Askenfelt. *Five lectures on the acoustics of the piano* (Stockholm : Royal Swedish Academy of Music), 1990.

[35]D. Thompson. *Railway Noise and Vibration: Mechanisms, Modelling and Means of Control* (Elsevier), 2009.

[36]K. L. Johnson. *Contact Mechanics* (Cambridge University Press, Cambridge), 1985.

[37]V. Popov. *Contact Mechanics and Friction: Physical Principles and Applications* (Springer), 2010.

[38]M. Ghosh. "An experimental study of the duration of contact of an elastic hammer striking a damped pianoforte string," Ind. J. Phys. **7**, 365-382 (1932)

[39]D. E. Hall. "Piano string excitation in the case of small hammer mass," J. Acoust. Soc. Am. **79**, 141-147 (1986)

[40]X. Boutillon. "Model for piano hammers: Experimental determination and digital simulation," J. Acoust. Soc. Am. **83**, 746 - 754 (1988)

[41]A. Chaigne, and A. Askenfelt. "Numerical simulations of piano strings. II. Comparisons with measurements and systematic exploration of some hammer-string parameters," J. Acoust. Soc. Am. **95** (1994)

[42]A. Stulov. "Hysteretic model of the grand piano hammer felt," J. Acoust. Soc. Am. **97** (1995)
[43]W. Brogan. "State variables and the state space description of dynamic systems," in *Modern Control Theory* (Prentice-Hall, 1985).
[44]J. Jiolat, C. d'Alessandro, J. L. Carrou, and J. Antunes. "Toward a physical model of the clavichord," J. Acoust. Soc. Am. **150**, 2350-2363 (2021)
[45]M. R. Schroeder. "New method of measuring reverberation time," J. Acoust. Soc. Am. **37**, 409-412 (1965)
[46]F. Fahy, and J. Walker. "Simple freely vibrating spring-mass system," in *Fundamentals of Noise and Vibration* (Spon Press, NY, USA, 1998).
[47]J. Chabassier. "Modélisation et simulation numérique d'un piano par modèles physiques," Docteur en Sciences dissertation, Ecole Polytechnique, Ecole Polytechnique,2012.
[48]J. Chabassier, and M. Durufle. "Physical parameters for piano modeling," (INRIA, 2012), p. 24.
[49]J. J. Tan. "Piano acoustics : string's double polarisation and piano source identification," PhD dissertation, Universite Paris Saclay,2018.
[50]A. Stulov. "Physical modelling of the piano string scale," Appl. Acoust. **69**, 977-984 (2008)
[51]Information on the copper density available at https://www.rsc.org/periodic-table/element/29/copper (Last viewed February, 2023)
[52]A. Chaigne, and A. Askenfelt. "Numerical simulations of piano strings. II. Comparisons with measurements and systematic exploration of some hammer-string parameters," J. Acoust. Soc. Am. **95**, 1631 - 1640 (1994)
[53]H. Conklin. "Design and tone in the mechanoacoustic piano. Part II. Piano structure," J. Acoust. Soc. Am. **100**, 695-708 (1996)
[54]C. F. T. Steinway. "Improvement in Duplex Agraffe Scales for Piano-Fortes", United States patent US126848A, 1872
[55]A. Askenfelt, and E. Jansson. "From touch to string vibrations. III: String motion and spectra," J. Acoust. Soc. Am. **93**, 2181-2196 (1993)
[56]R. Roy, and T. Kailath. "Esprit - estimation of signal parameters via rotational invariance techniques," IEEE Transactions on Acoustics Speech and Signal Processing **37**, 984-995 (1989)
[57]K. Ege, X. Boutillon, and B. David. "High-resolution modal analysis," J. Sound Vib. **4**, 852-869 (2009)